3-3-2023

# Optimal Identification of Unknown Parameters of Photovoltaic Models Using Dual-Population Gaining-Sharing Knowledge-Based Algorithm

Guojiang Xiong

*Guizhou Key Laboratory of Intelligent Technology in Power System, College of Electrical Engineering, Guizhou University, Guiyang 550025, China,Key Laboratory of Industrial Internet of Things & Networked Control, Ministry of Education, Chongqing 400065, China*

Lei Li

*Zunyi Power Supply Bureau, Guizhou Power Grid Co., Ltd., Zunyi 563000, China*

Ali Wagdy Mohamed

*Operations Research Department, Faculty of Graduate Studies for Statistical Research, Cairo University, Giza 12613, Egypt,Department of Mathematics and Actuarial Science, School of Sciences and Engineering, The American University in Cairo, Cairo, Egypt*

Jing Zhang

*Guizhou Key Laboratory of Intelligent Technology in Power System, College of Electrical Engineering, Guizhou University, Guiyang 550025, China*



## APA Citation

Xiong, G. Li, L. Mohamed, A. & Zhang, J. (2023). Optimal Identification of Unknown Parameters of Photovoltaic Models Using Dual-Population Gaining-Sharing Knowledge-Based Algorithm. *International Journal of Intelligent Systems, 2023*, 10.1155/2023/3788453
https://fount.aucegypt.edu/faculty_journal_articles/5533

## MLA Citation

Xiong, Guojiang, et al. "Optimal Identification of Unknown Parameters of Photovoltaic Models Using Dual-Population Gaining-Sharing Knowledge-Based Algorithm." *International Journal of Intelligent Systems,* vol. 2023, 2023,
https://fount.aucegypt.edu/faculty_journal_articles/5533

Hindawi
International Journal of Intelligent Systems
Volume 2023, Article ID 3788453, 24 pages
https://doi.org/10.1155/2023/3788453

WILEY | Hindawi

*Research Article*

# Optimal Identification of Unknown Parameters of Photovoltaic Models Using Dual-Population Gaining-Sharing Knowledge-Based Algorithm

**Guojiang Xiong,[1,2] Lei Li,[3] Ali Wagdy Mohamed,[4,5] Jing Zhang,[1] Yao Zhang,[6] and Hao Chen[7]**

[1]*Guizhou Key Laboratory of Intelligent Technology in Power System, College of Electrical Engineering, Guizhou University, Guiyang 550025, China*
[2]*Key Laboratory of Industrial Internet of Things & Networked Control, Ministry of Education, Chongqing 400065, China*
[3]*Zunyi Power Supply Bureau, Guizhou Power Grid Co., Ltd., Zunyi 563000, China*
[4]*Operations Research Department, Faculty of Graduate Studies for Statistical Research, Cairo University, Giza 12613, Egypt*
[5]*Department of Mathematics and Actuarial Science, School of Sciences and Engineering, The American University in Cairo, Cairo, Egypt*
[6]*Guizhou Electric Power Grid Dispatching and Control Center, Guiyang 550002, China*
[7]*Fujian Provincial Key Laboratory of Intelligent Identification and Control of Complex Dynamic System, Quanzhou 362216, China*

Correspondence should be addressed to Guojiang Xiong; gjxiongee@foxmail.com and Hao Chen; chenhao@fjirsm.ac.cn

Received 3 September 2022; Revised 19 November 2022; Accepted 21 November 2022; Published 3 March 2023

Academic Editor: Oscar Castillo



Establishing an accurate equivalent model is a critical foundation to describe the energy conversion characteristics of a photovoltaic system, which can support the research of fault analysis, output power prediction, and performance analysis of the photovoltaic system. However, the widely used equivalent models are highly nonlinear and have many unknown parameters, making it difficult to identify these parameters accurately. Our previous work found that the gaining-sharing knowledge-based algorithm (GSK) shows promising performance in solving this problem. But its efficacy is not enough to achieve accurate parameters within a relatively limited computing resource. In this context, a dual-population GSK algorithm (DPGSK), which introduces a dual-population evolution strategy for more excellent searchability, is proposed to address this issue. In each iteration, the population splits equally and randomly into two subpopulations, one of which performs the junior gaining-sharing phase while the other performs the senior gaining-sharing phase. Then two updated subpopulations merge to form a new population. This allows for a grand reconciliation of convergence speed and population diversity, giving DPGSK powerful optimization performance. Afterward, DPGSK is applied to five photovoltaic models and validated for performance against other advanced metaheuristics. Besides, the impact of different components on DPGSK is also investigated. Results and comparisons show that either component is indispensable to DPGSK, and DPGSK strengthens the convergence and achieves accurate and reliable results, demonstrating its superiority over other algorithms in solving this studied problem.

## 1. Introduction

As the most dominant contributor to current energy sources, fossil fuels, although cheap, versatile, and easy to store and transport, have resulted in climate change, environmental pollution, and even global warming as a result of their overuse [1–3]. Therefore, clean, green, and efficient renewable energy sources are urgently needed to curb the use of fossil energy. The renewable nature of solar, wind, geothermal, and biomass energy is self-explanatory. Among them, solar energy deserves to be used extensively as a universal, vast, and long-lasting clean energy due to its exclusive merits [4–6]. Photovoltaic (PV) is currently the primary form of utilization of solar power. To boost the efficiency of electrical energy conversion, it is highly essential to optimize the PV system accurately. As the electrical characteristics of a PV system are nonlinear, varying environments can affect the PV efficiency, leading to different performance parameters, and the parameters will also change in varying environments [7]. Thereby, accurate and effective modeling has become a significant and challenging problem in PV system optimization. To better design, predict, and estimate the performance of a PV system, an equivalent model to accurately characterize its energy transformation relationship is indispensable. The widely used equivalent models include the single/double diode models (SDM/DDM) [8–10]. SDM and DDM can help to understand the energy conversion behavior of PV systems and explain the dynamic voltage-current electrical characteristics. However, due to the existence of exponential and implicit functions, these two models are highly nonlinear and highly nonconvex. They contain five and seven unknown parameters, respectively, leading to difficulties in time consumption and low accuracy in achieving their optimal models. How to efficiently obtain accurate values for these models' unknown parameters is, therefore, a critical foundation for establishing the PV models.

At present, researchers have proposed various solutions to address this problem. Deterministic methods and metaheuristics can basically cover these solutions [8, 11]. The deterministic methods are further classified into analytical and numerical methods. The former deploys some particular measured points such as the maximum power and short-circuit and open-circuit moments to solve nonlinear equations to get unknown parameters [12–14]. The increase in the number of parameters impacts the modeling complexity and is time-consuming in the calculation. The analytical methods include the Lambert-W-based method [15], OSMP-based method [16], and reduced space search [17]. The numerical methods try to reduce the dimensionality of system equations by iterating all the experimental current and voltage data successively to solve the problem quickly. However, it applies only to continuous, differentiable, and convex functions [18]. In addition, initial values are crucial and unsuitable ones can lead to large errors in the identification results because these methods easily fall into local optimization. Therefore, the use of numerical methods has some limitations. The common numerical methods contain the Gauss–Seidel method [19], Newton-Raphson method [20], and the least-square method [21].

Deterministic methods rely heavily on functional models, which have severe defects such as sensitivity to initial solutions and easy to fall into local optimization. Thus, many metaheuristic algorithms derived from natural phenomena have been proposed to tackle various complex optimization problems including the studied problem [4, 22]. Each algorithm, however, has its own particular strengths and weaknesses. Particle swarm optimization (PSO) is a typical algorithm that is easy to realize and requires fewer parameters to coordinate, but it easily falls into local optimum and has insufficient search accuracy [23–25]. The cuckoo search algorithm (CS) is robust and not easily trapped in a local optimum, but it converges slowly [26]. Genetic algorithm (GA) converges fast but easily suffers from the problem of premature [27, 28]. Differential evolution (DE) is concise and valid but is strongly influenced by the algorithm parameters [29, 30]. Teaching-learning-based optimization (TLBO) is an easy-to-implement stochastic metaheuristic. However, its search capability is poor and the search accuracy is low [31]. The whale optimization algorithm (WOA) exploits the randomness of the best search agent to model the predation mechanisms. Nevertheless, its adaptive parameters depend on random distributions, and thereby it is prone to premature convergence [32]. Inspired by the intelligent behavior of bees, artificial bee colony optimization (ABC) avoids falling into local optima by employing operators to construct solutions randomly [33]. But it converges slowly and is hard to achieve satisfactory solutions within a limited resource. Motivated by the supply and demand mechanism, supply-demand-based optimization (SDO) combines different dynamic patterns of the spider web model organically to balance exploration and exploitation well [34]. However, its structure is slightly complex. In addition to the above-mentioned metaheuristic algorithms, many modified algorithms have also been proposed, such as the self-learning discrete jaya (SD-Jaya) [35], either-or TLBO (EOTLBO) [36], improved WOA (IWOA) [37], bee pollinator flower pollination algorithm (BPFPA) [38], classified perturbation mutation-based PSO (CPMPSO) [23], teaching-learning-based artificial bee colony (TLABC) [39], and Mixed-Variable Differential Evolution(MVDE) [40].

Undeniably, both the basic metaheuristic algorithms and their improved versions have shown excellent performance in tackling the PV models' parameter identification problem. Nevertheless, due to the problem's complexity and importance and the fact that it is not easy to obtain accurate values within a given limited computing resource, it is still a hard nut to crack. Besides, the no free lunch (NFL) theorem [41] points out emphatically that there is still a need to try and propose more methods with better performance to solve this concerned, tough optimization problem. Meanwhile, unlike the heuristic methods that rely on the characteristics of the specific problem to be solved, the metaheuristic algorithms achieve heuristic guidance through the exchange of information between population individuals and require less computational effort for large neighborhood search, and thus, can improve the search efficiency with the population-based iterated greedy mechanism [42]. Therefore, they are more popular to be applied to different complex engineering problems including the studied PV parameter identification.

Gaining-sharing knowledge-based algorithm (GSK) is another effective population-based metaheuristic algorithm [43]. Inspired by the two processes of knowledge gaining-sharing, GSK equips with two significant phases including junior/senior gaining-sharing, to prompt population individuals to evolve. The experimental results have shown the superior performance of GSK in solving benchmark optimization problems. Motivated by this, in one of our previous works, we applied the basic GSK successfully in tackling the

PV models' parameter identification problem for the first time [44]. The achieved results have demonstrated its good robustness and accuracy over other peer algorithms in this problem. However, we also found some shortcomings of GSK. On the one hand, the algorithm converges relatively slowly compared to other algorithms, especially in the early evolutionary stage. On the one hand, it is hard to achieve sufficiently accurate enough parameters within a relatively limited computing resource. The main reason is as follows: The original GSK algorithm relies primarily on the junior/senior gaining-sharing phases to weigh the exploration and exploitation. The first phase is mainly responsible for exploration, while the latter primarily supervises exploitation. In the early evolutionary stage, GSK tends to perform the junior phase, which leads to a slower convergence rate. In the later stage, the overwhelming adoption of the senior phase leads to a rapid decline in population diversity, which is not conducive to refining solutions with sufficient accuracy. Therefore, these two phases are not coordinated well enough to shape a powerful GSK in solving this problem.

In this paper, inspired by the distinct functional characteristics of these two phases, we propose an improved variant of GSK, namely, dual-population GSK (DPGSK), to tackle the studied problem. At the beginning of each iteration, the whole population is chopped up into two equal subpopulations randomly. One subpopulation employs the junior phase to update the corresponding individuals, while the other subpopulation adopts the senior phase to arm them. Finally, these two subpopulations merge to obtain a new population. This iterative approach can improve the convergence speed in the early stage, as only the senior phase is used in the first subpopulation. In the later stage, the population diversity is maintained as only the junior phase is used in the second subpopulation. The DPGSK algorithm's effectiveness is confirmed by comparing it with other algorithms in five models.

The motivations behind DPGSK are as follows:

(1) The original GSK contains two phases, and two subpopulations can select mutually exclusive phases to perform. However, in the original version, they are not well coordinated in different stages, leading to slow convergence in the early stage and a lack of adequate solution-refining capability in the later stage.
(2) The dual-population evolution strategy can achieve higher efficiency by updating two subpopulations in two distinct phases simultaneously.
(3) The dual-population can balance the population diversity and the convergence rate to avoid. This can compensate for poor convergence speed in the early stage and poor solution accuracy in the later stage. Therefore, exploration and exploitation can be equilibrated well to achieve accurate results.

The main contributions of this paper are listed as follows:

(1) An enhanced approach, namely, DPGSK is put forward to achieve accurate PV models' parameters.
(2) A dual-population evolution strategy is designed for DPGSK, by which each subpopulation selects one of the two phases of GSK to generate heterogeneous individuals to elevate the searchability of DPGSK.
(3) The suggested DPGSK algorithm is implemented in five PV models. The results highly confirm the superiority of DPGSK over other algorithms in solving the studied problem.

The remaining parts are outlined as follows: Section 2 presents the mathematical model of the studied problem. Sections 3 and 4 introduce the basic GSK algorithm and the proposed DPGSK, respectively. In Section 5, the analysis and discussions are summarized. Finally, Section 6 gives the conclusions.

## 2. Description of the PV Models

This section describes the SDM, DDM, and PV module models in detail. To establish the PV models more accurately, the model parameter identification problem is also formulated in this section.

*2.1. SDM.* Figure 1(a) is the circuital diagram of SDM. The total output voltage is $V_L$, and the output current $I_L$ is expressed as follows [45]:

$$I_L = I_{\mathrm{PV}} - I_D - I_{\mathrm{sh}} = I_{\mathrm{PV}} - I_{\mathrm{sd}}\left[\exp\left(\frac{q(V_L + I_L R_s)}{nkT}\right) - 1\right] - \frac{V_L + I_L R_s}{R_{\mathrm{sh}}}, \tag{1}$$

where $I_{\mathrm{PV}}$ means the photo-generated current, $I_D$ means the diode current, $I_{\mathrm{sh}}$ means shunt resistance current, $I_{\mathrm{sd}}$ means the saturation current, $n$ means the diode ideal factors, $k$ denotes the Boltzmann constant ($1.3806503 \times 10^{-23}$ J/K), $q$ denotes the electron charge ($1.60217646 \times 10^{-19}$ C), $T$ represents the PV cell temperature in Kelvin, $R_s$ is the series resistance, and $R_{\mathrm{sh}}$ is the parallel resistance.

As can be seen from the aforementioned parameters, the parameters identified in the SDM are $I_{\mathrm{PV}}$, $I_{\mathrm{sd}}$, $R_s$, $R_{\mathrm{sh}}$, and $n$.

*2.2. DDM.* Figure 1(b) is the circuital diagram of the DDM. The SDM ignores the recombination losses of current, while the DDM can solve this problem and guarantee a balance

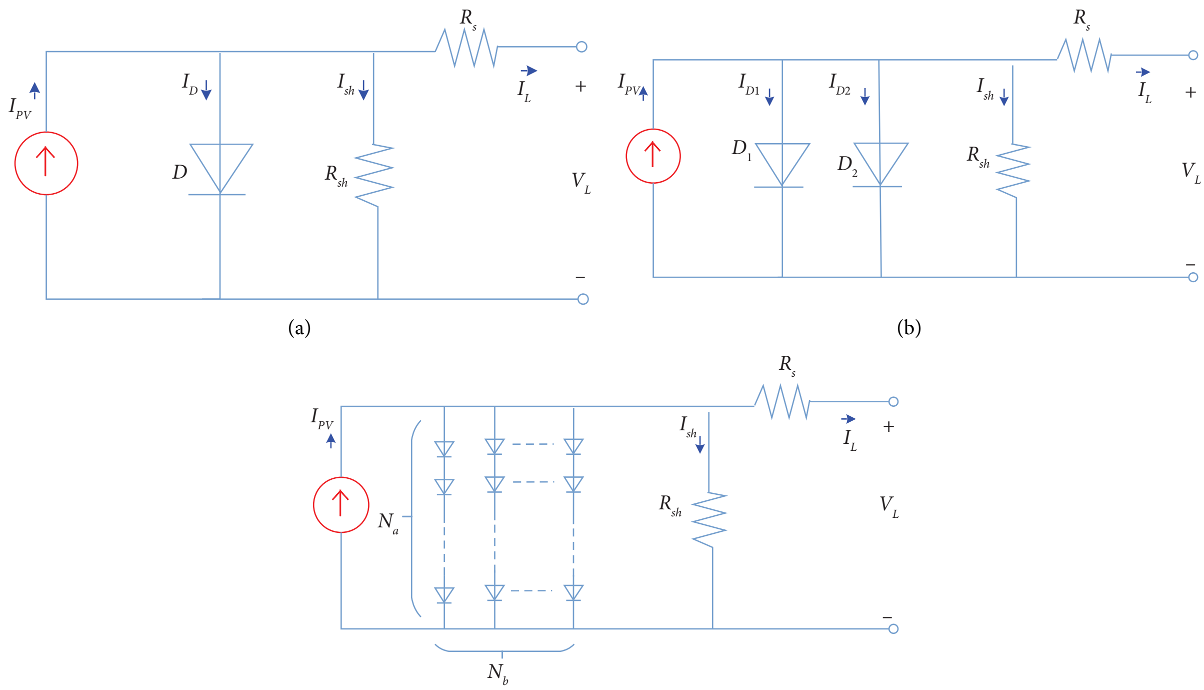


Figure 1: Circuits of PV models: (a) SDM; (b) DDM; (c) PV module.

between simplicity and accuracy. The $I_L$ is expressed as follows [46, 47]:

$$I_L = I_{\mathrm{PV}} - I_{D1} - I_{D2} - I_{\mathrm{sh}} = I_{\mathrm{PV}} - I_{\mathrm{sd1}}\left[\exp\left(\frac{q(V_L + I_L R_s)}{n_1 kT}\right) - 1\right] - I_{\mathrm{sd2}}\left[\exp\left(\frac{q(V_L + I_L R_s)}{n_2 kT}\right) - 1\right] - \frac{V_L + I_L R_s}{R_{\mathrm{sh}}}, \quad (2)$$

where $I_{D1}$ and $I_{D2}$ mean the first and second diode currents and $n_1$ and $n_2$ mean their corresponding ideal factors, respectively.

From (2), the parameters identified in the DDM are $I_{\mathrm{PV}}, I_{\mathrm{sd1}}, I_{\mathrm{sd2}}, R_s, R_{\mathrm{sh}}, n_1,$ and $n_2$.

*2.3. PV Module.* The circuital diagram of the PV module is given in Figure 1(c). It has $N_a \times N_b$ PV cells. $I_L$ is calculated as follows [48, 49]:

$$I_L = I_{\mathrm{PV}} N_b - I_{\mathrm{sd}} N_b\left[\exp\left(\frac{V_L + I_L R_s N_a/N_b}{n N_a V_t}\right) - 1\right] - \frac{V_L + I_L R_s N_a/N_b}{R_{\mathrm{sh}} N_a/N_b}. \quad (3)$$

From (3), the parameters identified in the PV module are $I_{\mathrm{PV}}, I_{\mathrm{sd}}, R_s, R_{\mathrm{sh}},$ and $n$, which are the same as the SDM.

*2.4. Objective Function.* In this work, we convert the studied problem into a numerical optimization problem, and use the root mean square error (RMSE) between the measured data and the calculated data as the objective function [50, 51].

$$\mathrm{RMSE}(x) = \sqrt{\frac{1}{N}\sum_{k=1}^{N} f(V_L, I_L, x)^2}, \quad (4)$$

where $N$ means the number of measured data. The error functions $f(V_L, I_L, x)$ and the solution vector $x$ are expressed as follows:

for the SDM,

$$\begin{cases} f(V_L, I_L, x) = I_{PV} - I_{sd}\left[\exp\left(\dfrac{q(V_L + I_L R_s)}{nkT}\right) - 1\right] - \dfrac{V_L + I_L R_s}{R_{sh}} - I_L, \\ x = (I_{\mathrm{PV}}, I_{sd}, R_s, I_{sh}, n), \end{cases} \tag{5}$$

for the DDM,

$$\begin{cases} f(V_L, I_L, x) = I_{PV} - I_{sd1}\left[\exp\left(\dfrac{q(V_L + I_L R_s)}{n_1 kT}\right) - 1\right] - I_{sd2}\left[\exp\left(\dfrac{q(V_L + I_L R_s)}{n_2 kT}\right) - 1\right] - \dfrac{V_L + I_L R_s}{R_{sh}} - I_L \\ x = (I_{PV}, I_{sd1}, I_{sd2}, R_s, I_{sh}, n_1, n_2) \end{cases}, \tag{6}$$

for the PV module,

$$\begin{cases} f(V_L, I_L, x) = I_{\mathrm{PV}} N_b - I_{sd} N_b\left[\exp\left(\dfrac{V_L + I_L R_s N_a / N_b}{n N_a V_t}\right) - 1\right] - \dfrac{V_L + I_L R_s N_a / N_b}{R_{sh} N_a / N_b} - I_L, \\ x = (I_{\mathrm{PV}}, I_{sd}, R_s, I_{sh}, n). \end{cases} \tag{7}$$

## 3. The Basic GSK Algorithm

GSK is a novel approach proposed for tackling optimization problems. According to the two processes of knowledge gaining-sharing, this algorithm comprises junior and senior gaining-sharing phases accordingly [43].

*3.1. Initialization.* In GSK, the population is made up of $Np$ individuals. The $i$-th individual $x_i$ is denoted as $x_i = (x_{i1}, x_{i2}, \cdots, x_{iD})$, where $D$ is the number of individual dimensions.

*3.2. Dimension Partitioning.* During the individual update process, $D_J$ denotes the number of dimensions an individual uses in the junior phase. $D_S$ denotes the rest that the individual uses in the senior phase. For an individual, an empirical equation is used to determine $D_J$ and $D_S$ as follows:

$$D_J = D \times \left(1 - \frac{G}{\mathrm{GEN}}\right)^K, \tag{8}$$

$$D_S = D - D_J, \tag{9}$$

where $K$ means the knowledge rate, $G$ means the generation number, and GEN means the required generation number.

*3.3. Junior Gaining-Sharing Phase.* For each individual in this phase, if the knowledge can be gained and shared, the updating formula is expressed as follows:

$$x_{i,\mathrm{new}} = \begin{cases} x_i + k_f \cdot \left[(x_{i-1} - x_{i+1}) + (x_r - x_i)\right], & \text{if } f(x_i) > f(x_r), \\ x_i + k_f \cdot \left[(x_{i-1} - x_{i+1}) + (x_i - x_r)\right], & \text{otherwise}, \end{cases} \tag{10}$$

where $k_f$ means the knowledge factor. $x_r$ is a random individual different from $x_{i-1}$, $x_i$ and $x_{i+1}$. $x_{i-1}$ and $x_{i+1}$ are selected by the following method:

Step 1: sort individuals in ascending order by their fitness values

Step 2: each individual $x_i$ selects two adjacent individuals including $x_{i-1}$ and $x_{i+1}$ to gain and share knowledge. The best $(x_{i-1})$ and worst $(x_{i+1})$ individuals are considered to be its adjacent individuals. For the best individual, the latter adjacent individuals are selected as follows: $x_1, x_2,$ *and* $x_3$. For the worst individual, the former adjacent individuals are selected as follows: $x_{Np-2}, x_{Np-1},$ and$x_{Np}$.

After generating $x_{i,\mathrm{new}}$, a parameter $k_r$ named knowledge ratio is adopted to regulate the probability of each update of an individual.

*3.4. Senior Gaining-Sharing Phase.* The update process in this phase is as follows:

$$x_{i,\mathrm{new}} = \begin{cases} x_i + k_f \cdot \left[\left(x_{p-\mathrm{best}} - x_{p-\mathrm{worst}}\right) + \left(x_m - x_i\right)\right], \text{if } f\left(x_i\right) > f\left(x_m\right), \\ x_i + k_f \cdot \left[\left(x_{p-\mathrm{best}} - x_{p-\mathrm{worst}}\right) + \left(x_i - x_m\right)\right], \text{otherwise}, \end{cases} \tag{11}$$

where $x_{p-\mathrm{best}}$, $x_{p-\mathrm{worst}}$, and $x_m$ are gaining and sharing sources different from $x_{i-1}$ and selected by the following method:

Step 1: sort individuals in ascending order by their fitness values and divide them into three groups, which are the best group (the top $100p\%$ individuals), the middle group (the medial $1 - 2 \times 100p\%$ individuals), and the worst group (the bottom $100p\%$ individuals), respectively

Step 2: for each individual $x_i$, the $x_{p-\mathrm{best}}$, $x_{p-\mathrm{worst}}$, and $x_m$ are randomly generated from the above three groups, respectively

The pseudocode of the GSK is given in Algorithm 1. *FEs* denotes the amount of fitness function, and Max _*FEs* denotes the upper limit of *FEs*.

## 4. The Proposed DPGSK

Although the original GSK works well on many optimization problems as a new type of metaheuristic algorithm, there is still room for improvement on a specific problem [44, 52, 53]. For example, in the studied problem in this paper, GSK has proven to have comprehensive performance in our previous study but still suffers from insufficient convergence and insufficient accuracy of solutions. Therefore, we purposefully propose an improved scheme to further raise its performance in the PV parameter identification problem.

It can be seen from the original GSK that an individual needs to refer to a lot of information to equip himself. Namely, the $D_J$ and $D_S$ dimensions of an individual choose to perform the junior and senior phases, respectively, which will perplex the movement of the individual toward the optimal solution. In this context, exploration and exploitation are hard to be coordinated well enough to shape GSK with a powerful search ability to tackle the PV models' parameter identification problem. This is mainly due to the relatively poor exploitation capacity in the early evolutionary stage when GSK mostly uses the junior phase. Moreover, GSK is gradually leaning towards the senior phase in the later stage, which leads to inadequate solution refining capability. Therefore, achieving highly-accurate parameters within a relatively limited computing resource is hard for GSK to solve this problem.

To conquer the shortcomings of GSK and balance exploration and exploitation, this work introduces a dual-population evolution strategy to obtain a dual-population GSK (DPGSK). In DPGSK, we randomly divide the population into two equal subpopulations **pop**1 and **pop**2 in each iteration. The first subpopulation, **pop**1, performs the junior gaining-sharing phase, while the other subpopulation, **pop**2, performs the senior gaining-sharing phase. After updating, these two subpopulations merge to obtain a new population. In this way, all dimensions of an individual refer to the same gaining and sharing sources to unify the movement to harmonize convergence and population diversity. DPGSK's flowchart is presented in Figure 2 and Algorithm 2.

## 5. Experimental Results

The proposed DPGSK algorithm is applied to five PV models, as shown in Table 1. Table 2 shows the parameters' range for these PV models [16, 54–56].

To better demonstrate DPGSK, we compare the algorithm with the basic GSK and other eight improved metaheuristic algorithms, which are the improved TLBO algorithm (ITLBO) [57], teaching-learning-based ABC algorithm (TLABC) [39], self-adaptive TLBO algorithm (SATLBO) [58], phasor PSO algorithm (PPSO) [59], comprehensive learning PSO algorithm (CLPSO) [60], improved JAYA optimization algorithm (IJAYA) [61], adaptive guided DE (AGDE) [62], and hybrid DE with WOA (DE_WOA) [63]. Table 3 shows the parameters setting for each algorithm. For the sake of fairness, all algorithms run individually 30 times in MATLAB R2018a.

*5.1. Results of the SDM.* The identification results of the five parameters of the SDM are shown in Table 4. After getting the solutions, they can be used to calculate the current data and individual absolute error values ($\mathrm{IAE} = |I_{L\ \mathrm{measured}} - I_{L\ \mathrm{calculated}}|$), presented in Table 5. We can see that the DPGSK's IAE (0.01769439) is consistently smaller than PPSO (0.01770360), AGDE (0.01770370), GSK (0.01770416), TLABC (0.01771991), ITLBO (0.01802719), and IJAYA (0.01806562). The current-voltage (I-V) and power-voltage (P-V) characteristic curves of DPGSK are plotted in Figure 3(a) and Figure 3(b), respectively, showing that a good agreement is found between the calculated data and the measured data. It demonstrates that DPGSK has superior accuracy in this model.

Table 6 shows the objective function values (RMSE) obtained by different algorithms in the SDM. To accurately verify the DPGSK's effectiveness, the best, worst, mean, and standard deviation (Std) values are used as reference indexes. The optimum values are highlighted in bold. DPGSK, GSK, AGDE, and DE_WOA obtain the smallest RMSE value

**Input**: algorithm parameters: NP, $k_f$, $k_r$, $K$, and $p$
**Output**: optimal solution
Set FEs = 0 and $G = 1$
Initialize a random population with NP individuals
Evaluate the objection function value for each individual
FEs = FEs + NP
**While** FEs < Max_FEs **do**
  **For** $i$ to NP**do**
    //Junior gaining-sharing phase
    Calculate $D_J$ with Equation (8)
    **For** $j = 1$ to $D_J$ **do**
      Generate $\boldsymbol{x}_{i.new}$ with Equation (10)
    **End**
    //Senior gaining-sharing phase
    Calculate the $D_S$ with Equation (9)
    **For** $j = 1$ to $D_S$ **do**
      Generate $\boldsymbol{x}_{i.new}$ with Equation (11)
    **End**
    Evaluate the objection function value for $\boldsymbol{x}_{i.new}$
    FEs = FEs + 1
    **If** $f(\boldsymbol{x}_{i.new}) \leq f(x_i)$ **then**
      $\boldsymbol{x}_i = \boldsymbol{x}_{i.new}$
    **End**
  **End**
  $G = G + 1$
**End while**

Algorithm 1: Basic GSK.

(9.86021878E-04), and DPGSK and GSK get the best mean value (9.86021878E-04). It is worth noting that DPGSK can get the optimal value (9.86021878E-04) in the worst index and the smallest value (5.01330110E-17) in the standard deviation. To analyze DPGSK's performance more fully, we used Wilcoxon's rank-sum test to validate it at a 0.05 confidence level. The $R^+$, $R^-$, and $p$ value result in Table 7 present that $R^+$ is notably higher than $R^-$, which shows the superior status of the presented DPGSK compared with other algorithms. Furthermore, the $p$ values are prominently below 0.05. In fact, the maximum $p$ value is only 2.43367962E-09, which is much smaller than the threshold value of 0.05. Therefore, the results in all indexes prove that DPGSK has the best search performance in the SDM.

In addition, Figure 4 gives all the above algorithms' convergence performance. It shows that DE_WOA converges the fastest in the early stage (before about 800 evaluations). However, after that, DPGSK exceeds DE_WOA, and it can find a better global optimal value instead of falling into a local optimal value. Furthermore, compared with GSK, the convergence speed of DPGSK is significantly improved, which demonstrates that the proposed dual-population evolution strategy indeed boosts the convergence of GSK considerably. In short, the DPGSK algorithm has excellent convergence in the SDM.

*5.2. Results of the DDM.* The identification results of the DDM are provided in Table 8. Table 9 and Figures 5(a) and 5(b) show the IAE results and characteristic curves achieved by DPGSK, respectively. We can see that the IAE value of DPGSK (0.01759995) is the smallest among all algorithms, indicating DPGSK is more competitive in the parameter identification accuracy of the DDM. Table 10 shows the RMSE values in the DDM, and DPGSK gets the best values in all the indexes (9.82484859E-04, 9.87885272E-04, 9.84815569E-04, and 1.68677548E-06, respectively). Table 11 shows the $R^+$, $R^-$, and $p$ values of Wilcoxon's rank-sum. Obviously, the values of $R^+$ are higher than those of $R^-$ consistently for all algorithms, and the $p$ values are all lower than 0.05 except for GSK. It indicates that DPGSK is significantly better than other algorithms and comparable to GSK. Therefore, it can conclude that DPGSK has a stronger search ability and robustness in the DDM. Moreover, the convergence curves in the DDM are presented in Figure 6. DE-WOA has the fastest convergence in the early stage but falls into local optimum quickly. DPGSK surpasses DE-WOA after about 2000 evaluations. The original GSK converges relatively slowly in the first half of the evolution, resulting in inaccurate values for the unknown parameters. In contrast, DPGSK has better overall convergence performance than other algorithms and searches for the global optimum more effectively.

*5.3. Results of the PV Modules.* The parameters identified for the Photowatt-PW201, STM6-40/36, and STP6-120/36 are listed in Tables 12–14, respectively. The IAE values are shown in Tables 15–17, and the characteristic curves are presented in Figures 7(a)–7(c), respectively. Moreover, Tables 18–20 show different algorithms' RMSE values, and

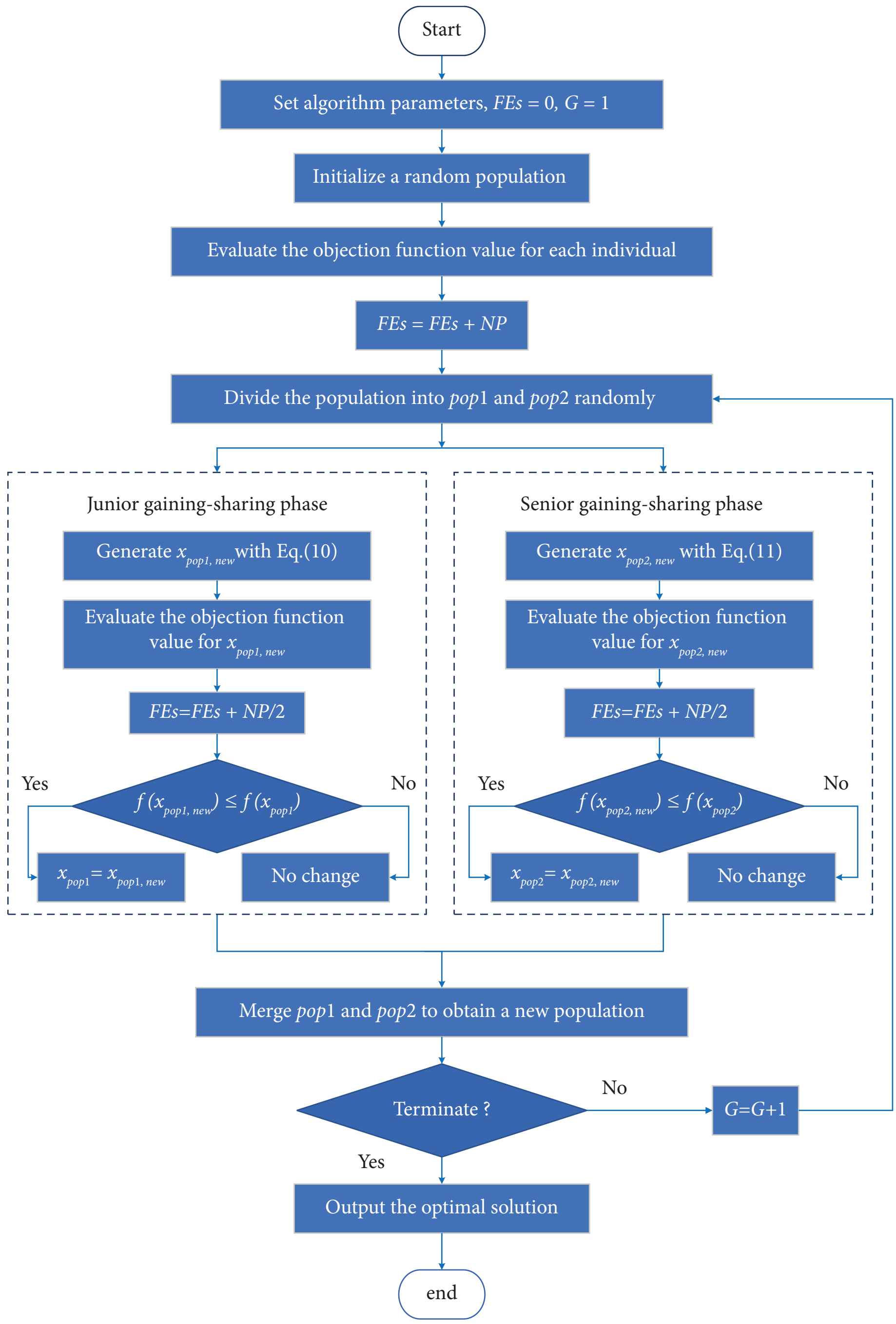


FIGURE 2: The flow chart of DPGSK.

Tables 21–23 show the $R^+$, $R^-$, and $p$ values of Wilcoxon's rank-sum test. Figures 8(a)–8(c) provide the convergence curves for these three PV modules, respectively.

*5.3.1. Analysis of the IAE Values.* Figures 7(a)–7(c) illustrate that the currents calculated by DPGSK fit the measured currents to a high degree. For the IAE results, DPGSK reaches the smallest IAE values in these modules. To be specific, the IAE values are 0.04153981, 0.06429210, and 0.27460349, respectively, demonstrating that DPGSK has higher accuracy in the parameter identification of these three PV modules than other algorithms.

*5.3.2. Analysis of the RMSE Values.* For the best RMSE index, in the Photowatt-PW201 module, DPGSK, GSK and AGDE yield the optimum result (2.42507487E-03). In the other two modules, four algorithms including DPGSK, GSK, AGDE, and DE_WOA, obtain the optimum values, which are 1.72981371E-03 and 1.66006031E-02, respectively.

For the worst RMSE index, DPGSK gets the optimum values in the Photowatt-PW201 and STP6-120/36, and the values are 2.42507487E-03 and 1.66006031E-02, respectively. For the STM6-40/36, both DPGSK and DE_WOA achieve the same optimum value (1.72981371E-03).

```
Input: algorithm parameters: NP, k_f, k_r, and p
Output: optimal solution
Set FEs = 0 and G = 1
Initialize a random population with NP individuals
Evaluate the objection function value for each individual
FEs = FEs + NP
While FEs < Max_FEs do
    Divide the population into pop1 and pop2 randomly
    //Junior gaining-sharing phase (for pop1)
    For i = 1 to NP/2do
        Generate x_{pop1, i, new} with Equation (10)
        Evaluate the objection function value for x_{pop1, i, new}
        FEs = FEs + 1
        If f (x_{pop1, i, new}) ≤ f (x_{pop1, i}), then
            x_{pop1, i} = x_{pop1, i, new}
        End
    End
    //Senior gaining-sharing phase (for pop2)
    For i = 1 to NP/2do
        Generate x_{pop2, i, new} with Equation (11)
        Evaluate the objection function value for x_{pop2, i, new}
        FEs = FEs + 1
        If f (x_{pop2,i,new}) ≤ f (x_{pop2,i}) then
            x_{pop2,i} = x_{pop2,i,new}
        End
    End
    Merge pop1 and pop2 to obtain a new population
    G = G + 1
End while
```

ALGORITHM 2: Proposed DPGSK.

TABLE 1: Five models' information.

| PV model | Solar cell Type | Solar cell Number | Irradiance (W/m$^2$) | Temperature (°C) | Max_FEs |
|---|---|---|---|---|---|
| SDM/DDM | RT.C. France silicon solar cell | 1 | 1000 | 33 | 10000 |
| Photowatt-PWP201 | Polysilicon cell | 36 | 1000 | 45 | 10000 |
| STM6-40/36 | Monocrystalline silicon cell | 36 | 1000 | 51 | 15000 |
| STP6-120/36 | Monocrystalline silicon cell | 36 | 1000 | 55 | 15000 |

TABLE 2: PV models' parameters range.

| Parameter | Single/double diode | | Photowatt-PW201 | | STM6-40/36 | | STP6-120/36 | |
|---|---|---|---|---|---|---|---|---|
| | LB | UB | LB | UB | LB | UB | LB | UB |
| $I_{ph}$ (A) | 0 | 1 | 0 | 2 | 0 | 2 | 0 | 8 |
| $I_{sd}$, $I_{sd1}$, $I_{sd2}$ ($\mu$A) | 0 | 1 | 0 | 50 | 0 | 50 | 0 | 50 |
| $R_s$ ($\Omega$) | 0 | 0.5 | 0 | 2 | 0 | 0.36 | 0 | 0.36 |
| $R_{sh}$ ($\Omega$) | 0 | 100 | 0 | 2000 | 0 | 1000 | 0 | 1500 |
| $n$, $n_1$, $n_2$ | 1 | 2 | 1 | 50 | 1 | 60 | 1 | 50 |

For the mean RMSE index, DPGSK yields the optimum values, i.e., 2.42507487E-03 and 1.66006031E-02, respectively, in the Photowatt-PW201 and STP6-120/36 modules. For the STM6-40/36 module, DPGSK, GSK, and DE_WOA reach the same optimum value (1.72981371E-03).

For the standard deviation, only DPGSK provides the best performance in all the three PV modules. The values are 4.75324029E-17, 6.69268329E-18, and 3.64215013E-16, respectively. Particularly, the optimal standard deviation values of DPGSK are significantly better than that of others.

Table 3: Parameters setting.

| Algorithm | Parameter setting |
|---|---|
| DPGSK | NP = 20, $k_r = 0.9$, $k_f = 0.5$, $p = 0.1$ |
| GSK | NP = 20, $k_r = 0.9$, $k_f = 0.5$, $K = 10$, $p = 0.1$ |
| ITLBO | NP = 20 |
| SATLBO | NP = 20 |
| TLABC | NP = 20, $F$ = rand (0,1) |
| IJAYA | NP = 20 |
| PPSO | NP = 20 |
| CLPSO | NP = 20, gap = 7, $c = 1.49445$, $w = 0.9$ to 0.4 |
| AGDE | NP = 20, part_size = 0.1 |
| DE_WOA | NP = 20, $F$ = rand (0.1,1), CR = rand (0,1) |

Table 4: Parameter identification results of the SDM.

| Algorithm | Parameter | | | | |
|---|---|---|---|---|---|
| | $I_{ph}$ (A) | $I_{sd}$ ($\mu$A) | $R_s$ ($\Omega$) | $R_{sh}$ ($\Omega$) | $n$ |
| DPGSK | 0.76077553 | 0.32302079 | 0.03637709 | 53.71852013 | 1.48118358 |
| GSK | 0.76077553 | 0.32302085 | 0.03637709 | 53.71852481 | 1.48118360 |
| ITLBO | 0.76088942 | 0.30531731 | 0.03658155 | 51.11235228 | 1.47555381 |
| SATLBO | 0.76098523 | 0.33649797 | 0.03621845 | 53.24192945 | 1.48531569 |
| TLABC | 0.76074567 | 0.32115398 | 0.03639442 | 53.76527575 | 1.48060283 |
| IJAYA | 0.76083168 | 0.29010861 | 0.03678511 | 52.18389372 | 1.47039884 |
| PPSO | 0.76076441 | 0.33383560 | 0.03624545 | 54.58985322 | 1.48450689 |
| CLPSO | 0.76098396 | 0.370652361 | 0.03492495 | 57.25728241 | 1.49542141 |
| AGDE | 0.76077548 | 0.32303137 | 0.03637697 | 53.72031579 | 1.48118683 |
| DE_WOA | 0.76077552 | 0.32302447 | 0.03637705 | 53.71869823 | 1.48118474 |

Table 5: IAE results in the SDM.

| Item | $V_L$ (V) | $I_{L\text{measured}}$ (A) | $I_{L\text{calculated}}$ (A) | | | | | | |
|---|---|---|---|---|---|---|---|---|---|
| | | | DPGSK | GSK | ITLBO | TLABC | IJAYA | PPSO | AGDE |
| 1 | −0.2057 | 0.7640 | 0.76402556 | 0.76408765 | 0.76436713 | 0.76405468 | 0.76423508 | 0.76408764 | 0.76408749 |
| 2 | −0.1291 | 0.7620 | 0.76262328 | 0.76266264 | 0.76286952 | 0.76263091 | 0.76276822 | 0.76266264 | 0.76266253 |
| 3 | −0.0588 | 0.7605 | 0.76133622 | 0.76135473 | 0.76149499 | 0.76132414 | 0.76142189 | 0.76135472 | 0.76135466 |
| 4 | 0.0057 | 0.7605 | 0.76015484 | 0.76015423 | 0.76023338 | 0.76012468 | 0.76018618 | 0.76015427 | 0.76015420 |
| 5 | 0.0646 | 0.7600 | 0.75907387 | 0.75905585 | 0.75907929 | 0.75902727 | 0.75905582 | 0.75905635 | 0.75905586 |
| 6 | 0.1185 | 0.7590 | 0.75807680 | 0.75804300 | 0.75801572 | 0.75801534 | 0.75801419 | 0.75804300 | 0.75804305 |
| 7 | 0.1678 | 0.7570 | 0.75713938 | 0.75709159 | 0.75701864 | 0.75706483 | 0.75703780 | 0.75709159 | 0.75709166 |
| 8 | 0.2132 | 0.7570 | 0.75620170 | 0.75614207 | 0.75602889 | 0.75611634 | 0.75606865 | 0.75614207 | 0.75614217 |
| 9 | 0.2545 | 0.7555 | 0.75515544 | 0.75508732 | 0.75494149 | 0.75506296 | 0.75500327 | 0.75508732 | 0.75508744 |
| 10 | 0.2924 | 0.7540 | 0.75373601 | 0.75366447 | 0.75349632 | 0.75364218 | 0.75358460 | 0.75366447 | 0.75366460 |
| 11 | 0.3269 | 0.7505 | 0.75145540 | 0.75138806 | 0.75121264 | 0.75136907 | 0.75133542 | 0.75138806 | 0.75138820 |
| 12 | 0.3585 | 0.7465 | 0.74740107 | 0.74734834 | 0.74718587 | 0.74733452 | 0.74735513 | 0.74734834 | 0.74734848 |
| 13 | 0.3873 | 0.7385 | 0.74012294 | 0.74009688 | 0.73997134 | 0.74009054 | 0.74020040 | 0.74009688 | 0.74009699 |
| 14 | 0.4137 | 0.7280 | 0.72738539 | 0.72739678 | 0.72733136 | 0.72740028 | 0.72762993 | 0.72739678 | 0.72739686 |
| 15 | 0.4373 | 0.7065 | 0.70690114 | 0.70695327 | 0.70695979 | 0.70696778 | 0.70732358 | 0.70695327 | 0.70695331 |
| 16 | 0.4590 | 0.6755 | 0.67520863 | 0.67529489 | 0.67536910 | 0.67531996 | 0.67577635 | 0.67529490 | 0.67529488 |
| 17 | 0.4784 | 0.6320 | 0.63078292 | 0.63088431 | 0.63100001 | 0.63091697 | 0.63140894 | 0.63088431 | 0.63088426 |
| 18 | 0.4960 | 0.5730 | 0.57199009 | 0.57208207 | 0.57220153 | 0.57211788 | 0.57256254 | 0.57208207 | 0.57208200 |
| 19 | 0.5119 | 0.4990 | 0.49943067 | 0.49949164 | 0.49957875 | 0.49952593 | 0.49984987 | 0.49949164 | 0.49949157 |
| 20 | 0.5265 | 0.4130 | 0.41347542 | 0.41349356 | 0.41352576 | 0.41352273 | 0.41368331 | 0.41349356 | 0.41349350 |
| 21 | 0.5398 | 0.3165 | 0.31724244 | 0.31721950 | 0.31719456 | 0.31724187 | 0.31724001 | 0.31721950 | 0.31721946 |
| 22 | 0.5521 | 0.2120 | 0.21215403 | 0.21210317 | 0.21203682 | 0.21211888 | 0.21199141 | 0.21210317 | 0.21210313 |
| 23 | 0.5633 | 0.1035 | 0.10277871 | 0.10272135 | 0.10264290 | 0.10273211 | 0.10254314 | 0.10272134 | 0.10272129 |
| 24 | 0.5736 | −0.0100 | −0.00920948 | −0.00924886 | −0.00930440 | −0.00924053 | −0.00941687 | −0.00924887 | −0.00924895 |
| 25 | 0.5833 | −0.1230 | −0.12438567 | −0.12438137 | −0.12437645 | −0.12437260 | −0.12445883 | −0.12438137 | −0.12438151 |
| 26 | 0.5900 | −0.2100 | −0.20924496 | −0.20919304 | −0.20912068 | −0.20918205 | −0.20915470 | −0.20919304 | −0.20919323 |
| | $\sum$ IAE | | **0.01769439** | 0.01770416 | 0.01802719 | 0.01771991 | 0.01806562 | 0.01770360 | 0.01770370 |

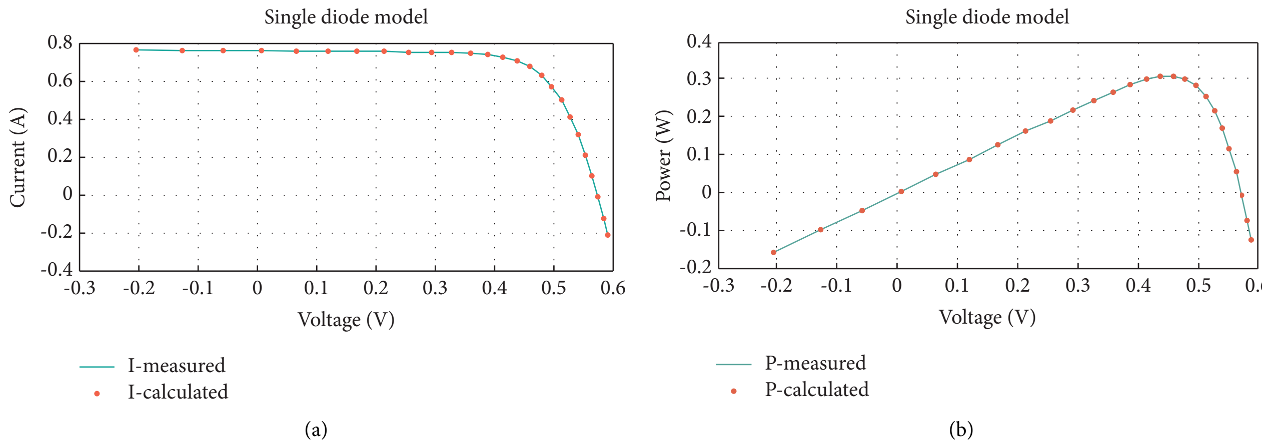


Figure 3: Characteristic curves of DPGSK in the SDM. (a) I-V. (b) P-V.

Table 6: RMSE values in the SDM.

| Algorithm | RMSE | | | |
|---|---|---|---|---|
| | Best | Worst | Mean | Std |
| DPGSK | **9.86021878E − 04** | **9.86021878E − 04** | **9.86021878E − 04** | **5.01330110E − 17** |
| GSK | **9.86021878E − 04** | 9.86021881E − 04 | **9.86021878E − 04** | 5.77198278E − 13 |
| ITLBO | 9.86942857E − 04 | 2.75231746E − 03 | 1.33505454E − 03 | 3.77679086E − 04 |
| SATLBO | 9.97038389E − 04 | 4.00809225E − 03 | 1.73821140E − 03 | 7.96717306E − 04 |
| TLABC | 9.86040588E − 04 | 2.09497050E − 03 | 1.15942131E − 03 | 2.34420712E − 04 |
| IJAYA | 9.95090806E − 04 | 1.52426755E − 03 | 1.15901344E − 03 | 1.52354222E − 04 |
| PPSO | 9.86716093E − 04 | 3.96453377E − 03 | 1.65111091E − 03 | 7.01783183E − 04 |
| CLPSO | 1.31226121E − 03 | 4.67174715E − 03 | 2.48297876E − 03 | 7.74142094E − 04 |
| AGDE | **9.86021878E − 04** | 1.40212898E − 03 | 1.00260688E − 03 | 7.67404144E − 05 |
| DE_WOA | **9.86021878E − 04** | 9.86024119E − 04 | 9.86021990E − 04 | 4.37393539E − 10 |

The optimum values are highlighted in bold.

Table 7: $R^+$, $R^-$, and $p$ values of Wilcoxon's rank-sum test for the RMSE values of the DPGSK vs. other algorithms in the SDM.

| DPGSK vs. | $R^+$ | $R^-$ | $p$ value | Sig. |
|---|---|---|---|---|
| GSK | 1355.50 | 474.50 | 7.74308961E − 11 | ↑ |
| ITLBO | 1365.00 | 465.00 | 3.01418492E − 11 | ↑ |
| SATLBO | 1365.00 | 465.00 | 3.01418492E − 11 | ↑ |
| TLABC | 1365.00 | 465.00 | 3.01418492E − 11 | ↑ |
| IJAYA | 1365.00 | 465.00 | 3.01418492E − 11 | ↑ |
| PPSO | 1365.00 | 465.00 | 3.01418492E − 11 | ↑ |
| CLPSO | 1365.00 | 465.00 | 3.01418492E − 11 | ↑ |
| AGDE | 1364.00 | 466.00 | 3.33006361E − 11 | ↑ |
| DE_WOA | 1319.00 | 511.00 | 2.43367962E − 09 | ↑ |

The sign "↑" means that DPGSK is significantly superior to the compared competitor.

The above comparisons fully indicate that DPGSK obtains the most accurate parameters' values for the three PV modules and shows the strongest robustness in searching for the global optimal solutions.

*5.3.3. Analysis of the Convergence Performance.* In the Photowatt-PW201 module, DPGSK and DE-WOA converge faster than other algorithms during the initial stage (before about 1000 evaluations). Moreover, compared with GSK, DPGSK improves the convergence performance effectively. In the last two modules, DE-WOA converges fastest, and DPGSK converges similarly to GSK. In the STM6-40/36 module, DPGSK surpasses DE-WOA at approximately 4000 evaluations. In the STP6-120/36 module, DPGSK completely surpasses GSK at approximately 3000 evaluations and surpasses DE-WOA at approximately 6000 evaluations. DE-WOA falls into local convergence in all the PV modules, while DPGSK can avoid the local optimum effectively and surpass GSK to search for the global optimum. Therefore, it proves again that DPGSK has stronger competitiveness in convergence performance.

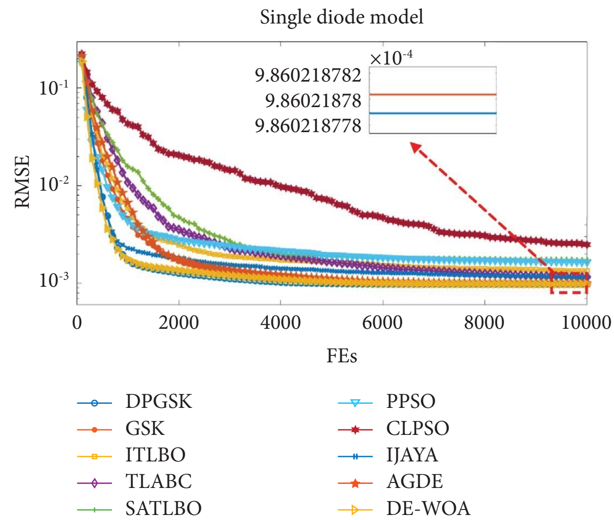


FIGURE 4: Convergence curves in the SDM.

TABLE 8: Parameter identification results of the DDM.

| Algorithm | Parameter | | | | | | |
|---|---|---|---|---|---|---|---|
| | $I_{ph}$ (A) | $I_{sd1}$ ($\mu$A) | $I_{sd2}$ ($\mu$A) | $R_s$ ($\Omega$) | $R_{sh}$ ($\Omega$) | $n_1$ | $n_2$ |
| DPGSK | 0.76077168 | 0.25583590 | 0.11052916 | 0.03644723 | 54.01092626 | 1.46639593 | 1.64126723 |
| GSK | 0.76077847 | 0.17092238 | 0.26394496 | 0.03648583 | 54.28926304 | 1.76856035 | 1.46597779 |
| ITLBO | 0.76077553 | 0.14239269 | 0.18110179 | 0.03637850 | 53.72272176 | 1.48849728 | 1.47607649 |
| SATLBO | 0.76096271 | 0.40876719 | 0.16662876 | 0.03648058 | 54.25291092 | 1.70980158 | 1.43554851 |
| TLABC | 0.76084150 | 0.14106070 | 0.39227701 | 0.03679306 | 54.15110002 | 1.42305668 | 1.68539145 |
| IJAYA | 0.76079609 | 0.23469918 | 0.21099112 | 0.03651187 | 54.73346624 | 1.68421377 | 1.45209458 |
| PPSO | 0.76083767 | 0.10308949 | 0.60945205 | 0.03760498 | 52.22118743 | 1.39259550 | 1.75664548 |
| CLPSO | 0.76077382 | 0.04056545 | 0.16670401 | 0.04103186 | 51.35048578 | 1.31412732 | 1.58710667 |
| AGDE | 0.76084759 | 0.11467499 | 0.21581341 | 0.03643901 | 52.88962572 | 1.53128949 | 1.46569019 |
| DE_WOA | 0.76078731 | 0.38618205 | 0.10301104 | 0.03677098 | 54.69665473 | 1.62937670 | 1.40773189 |

*5.3.4. Analysis of the Test Results.* The test outcomes provided in Tables 21–23 reveal that all the $R^+$ values are clearly higher than the $R^-$ values. For most methods, the $R^+$ is 1365, and only the $R^+$ of DE-WOA is 1327.5 in the Photowatt-PW201 module. The $R^+$ of GSK and DE-WOA in the STM6-40/36 module are 1356.5 and 1341, respectively. In the STP6-120/36 module, GSK and DE-WOA have an $R^+$ of 1356.5 and 1341, respectively. Obviously, in these three modules, the $p$ values are considerably below 0.05, indicating that DPGSK significantly outperforms all the other methods. It concludes that the suggested DPGSK is statistically more reliable than other competitors.

*5.4. Whole Performance.* The DPGSK algorithm is compared with other algorithms in different models separately above. However, its performance could not be verified comprehensively by the experimental results in a single model. Therefore, the Friedman test is employed here for the statistical analysis of multiple models simultaneously at a confidence level of 0.05. The test results, as displayed in Figure 9, demonstrate that DPGSK ranks first with an average ranking of 1.40, followed by GSK, DE_WOA, AGDE, IJAYA, TLABC, PPSO, ITLBO, SATLBO, and CLPSO, which further indicates the superior status of the presented algorithm over others.

*5.5. Analysis of the Components.* It is known that GSK contains two phases, i.e., the junior and the senior. In the proposed DPGSK, it adopts the dual-population evolution strategy to divide the senior and junior phases into two random subpopulations of equal size. In this subsection, the effect of each phase on DPGSK is evaluated. Two variants are considered. One variant that only uses the junior phase is IGSK1, and the other variant that only performs the senior phase is IGSK2.

*5.5.1. Analysis of the RMSE Values.* For the best RMSE indicator, all four algorithms get the optimum values 9.86021878E-04 and 2.42507487E-03 in the SDM and the Photowatt-PW201 module, respectively, as shown in Table 24. In the DDM, IGSK2 gets the best value (9.82484852E-04), and DPGSK's value (9.82484859E-04) stays close behind IGSK2. In the STM6-40/36 and STP6-120/36 modules, DPGSK, GSK, and IGSK2 obtain the same optimum values, which are 1.72981371E-03 and 1.66006031E-02, respectively.

Table 9: IAE results in the DDM.

| Item | $V_L$ (V) | $I_{L\text{measured}}$ (A) | $I_{L\text{calculated}}$ (A) | | | | | | |
|---|---|---|---|---|---|---|---|---|---|
| | | | DPGSK | GSK | ITLBO | TLABC | IJAYA | PPSO | AGDE |
| 1 | −0.2057 | 0.7640 | 0.76404493 | 0.76405437 | 0.76408737 | 0.76412147 | 0.76404506 | 0.76422705 | 0.76421064 |
| 2 | −0.1291 | 0.7620 | 0.76264663 | 0.76264432 | 0.76266247 | 0.76270783 | 0.76264646 | 0.76276121 | 0.76276331 |
| 3 | −0.0588 | 0.7605 | 0.76134678 | 0.76135011 | 0.76135466 | 0.76141028 | 0.76136273 | 0.76141570 | 0.76143492 |
| 4 | 0.0057 | 0.7605 | 0.76015271 | 0.76016206 | 0.76015425 | 0.76021906 | 0.76018428 | 0.76018028 | 0.76021561 |
| 5 | 0.0646 | 0.7600 | 0.75906006 | 0.75907473 | 0.75905596 | 0.75912848 | 0.75910566 | 0.75904889 | 0.75910005 |
| 6 | 0.1185 | 0.7590 | 0.75805209 | 0.75807121 | 0.75804319 | 0.75812109 | 0.75810989 | 0.75800317 | 0.75807141 |
| 7 | 0.1678 | 0.7570 | 0.75710434 | 0.75712665 | 0.75709182 | 0.75717100 | 0.75717191 | 0.75701636 | 0.75710543 |
| 8 | 0.2132 | 0.7570 | 0.75615666 | 0.75618033 | 0.75614233 | 0.75621582 | 0.75623053 | 0.75602526 | 0.75614234 |
| 9 | 0.2545 | 0.7555 | 0.75510107 | 0.75512352 | 0.75508757 | 0.75514495 | 0.75517617 | 0.75492077 | 0.75507511 |
| 10 | 0.2924 | 0.7540 | 0.75366391 | 0.75369196 | 0.75366466 | 0.75369265 | 0.75374364 | 0.75344150 | 0.75364091 |
| 11 | 0.3269 | 0.7505 | 0.75138959 | 0.75140000 | 0.75138812 | 0.75137426 | 0.75144661 | 0.75111331 | 0.75135496 |
| 12 | 0.3585 | 0.7465 | 0.74733934 | 0.74733975 | 0.74734825 | 0.74728651 | 0.74737732 | 0.74704911 | 0.74730858 |
| 13 | 0.3873 | 0.7385 | 0.74007737 | 0.74006754 | 0.74009662 | 0.73999500 | 0.74009380 | 0.73983240 | 0.74005480 |
| 14 | 0.4137 | 0.7280 | 0.72737048 | 0.72735306 | 0.72739641 | 0.72728047 | 0.72736897 | 0.72725349 | 0.72735795 |
| 15 | 0.4373 | 0.7065 | 0.70688719 | 0.70690744 | 0.70695291 | 0.70686026 | 0.70691820 | 0.70701042 | 0.70692291 |
| 16 | 0.4590 | 0.6755 | 0.67527661 | 0.67526034 | 0.67529466 | 0.67526010 | 0.67527383 | 0.67558755 | 0.67527618 |
| 17 | 0.4784 | 0.6320 | 0.63087826 | 0.63086933 | 0.63088427 | 0.63091974 | 0.63089314 | 0.63135733 | 0.63087640 |
| 18 | 0.4960 | 0.5730 | 0.57208764 | 0.57208659 | 0.57208221 | 0.57217132 | 0.57212484 | 0.57260736 | 0.57208087 |
| 19 | 0.5119 | 0.4990 | 0.49950384 | 0.49950813 | 0.49949187 | 0.49959773 | 0.49955993 | 0.49991695 | 0.49949193 |
| 20 | 0.5265 | 0.4130 | 0.41350590 | 0.41351180 | 0.41349377 | 0.41357743 | 0.41357227 | 0.41370317 | 0.41349169 |
| 21 | 0.5398 | 0.3165 | 0.31722685 | 0.31723122 | 0.31721961 | 0.31725638 | 0.31729325 | 0.31717851 | 0.31721518 |
| 22 | 0.5521 | 0.2120 | 0.21210344 | 0.21210483 | 0.21210315 | 0.21208974 | 0.21216130 | 0.21186020 | 0.21209971 |
| 23 | 0.5633 | 0.1035 | 0.10271591 | 0.10271488 | 0.10272123 | 0.10267609 | 0.10276008 | 0.10239586 | 0.10272483 |
| 24 | 0.5736 | −0.0100 | −0.00925611 | −0.00925748 | −0.00924897 | −0.00923317 | −0.00922742 | −0.00950125 | −0.00923084 |
| 25 | 0.5833 | −0.1230 | −0.12438481 | −0.12438340 | −0.12438136 | −0.12438285 | −0.12437102 | −0.12438554 | −0.12434028 |
| 26 | 0.5900 | −0.2100 | −0.20918955 | −0.20918379 | −0.20919287 | −0.20913412 | −0.20918506 | −0.20890333 | −0.20912974 |
| | $\sum$ IAE | | **0.01759995** | 0.01760029 | 0.01770340 | 0.01763368 | 0.01763637 | 0.01769859 | 0.01787209 |

The optimum values are highlighted in bold.

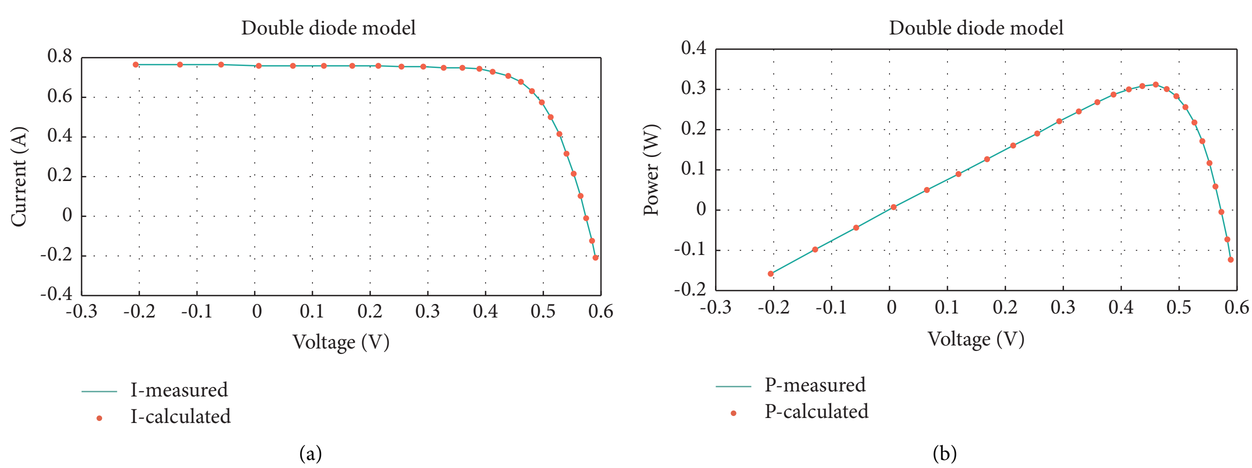


Figure 5: Characteristic curves of DPGSK in the DDM: (a) I-V and (b) P-V.

For the worst RMSE indicator, DPGSK and IGSK2 get the optimum values in the SDM and STM6-40/36 module, which are 9.86021878E-04 and 1.72981371E-03, respectively. In the DDM, Photowatt-PW201 module, and STP6-120/36 module, only DPGSK achieves the optimum values, i.e., 9.87885272E-04, 2.42507487E-03, and 1.66006031E-02, respectively.

For the mean RMSE indicator, DPGSK, GSK, and IGSK2 get the optimum values in the SDM and STM6-40/36 module and the values are 9.86021878E-04 and 1.72981371E-03, respectively. In the DDM, Photowatt-PW201 module, and STP6-120/36 module, only DPGSK achieves the optimum values, i.e., 9.84815569E-04, 2.42507487E-03, and 1.66006031E-02, respectively.

For the standard deviation, DPGSK achieves the optimum values in the DDM, Photowatt-PW201, STM6-40/36, and STP6-120/36 modules, which are 1.68677548E-06, 4.75324029E-17, 6.69268329E-18, and 3.64215013E-16,

Table 10: RMSE values in the DDM.

| Algorithm | RMSE | | | |
|---|---|---|---|---|
| | Best | Worst | Mean | Std |
| DPGSK | **9.82484859E – 04** | **9.87885272E – 04** | **9.84815569E – 04** | **1.68677548E – 06** |
| GSK | 9.82681198*E* – 04 | 9.91166708*E* – 04 | 9.85246463*E* – 04 | 1.78610712*E* – 06 |
| ITLBO | 9.84345253E – 04 | 4.31097698*E* – 03 | 1.75430730*E* – 03 | 8.04653832*E* – 04 |
| SATLBO | 9.90006061*E* – 04 | 2.98794798*E* – 03 | 1.71833393*E* – 03 | 5.73888171*E* – 04 |
| TLABC | 9.85002657*E* – 04 | 2.31622995*E* – 03 | 1.32240610*E* – 03 | 3.65025331*E* – 04 |
| IJAYA | 9.86676609*E* – 04 | 2.12261011*E* – 03 | 1.31023130*E* – 03 | 2.60436562*E* – 04 |
| PPSO | 9.87968584*E* – 04 | 2.78834805*E* – 03 | 1.62052853*E* – 03 | 5.06325501*E* – 04 |
| CLPSO | 1.53872824*E* – 03 | 4.52312248*E* – 03 | 2.99124493*E* – 03 | 7.37512494*E* – 04 |
| AGDE | 9.82862593*E* – 04 | 1.84667496*E* – 03 | 1.07310473*E* – 03 | 2.00132037*E* – 04 |
| DE_WOA | 9.83101057*E* – 04 | 1.36161947*E* – 03 | 1.01475307*E* – 03 | 7.93377243*E* – 05 |

The optimum values are highlighted in bold.

Table 11: $R^+$, $R^-$, and $p$ values of Wilcoxon's rank-sum test for the RMSE values of the DPGSK vs. other algorithms in the DDM.

| DPGSK vs. | $R^+$ | $R^-$ | $p$ value | Sig. |
|---|---|---|---|---|
| GSK | 974.00 | 856.00 | 3.87099778*E* – 01 | ≈ |
| ITLBO | 1333.00 | 497.00 | 6.72195436*E* – 10 | ↑ |
| SATLBO | 1365.00 | 465.00 | 3.01985936*E* – 11 | ↑ |
| TLABC | 1344.00 | 486.00 | 2.37146943*E* – 10 | ↑ |
| IJAYA | 1362.00 | 468.00 | 4.07716485*E* – 11 | ↑ |
| PPSO | 1365.00 | 465.00 | 3.01985936*E* – 11 | ↑ |
| CLPSO | 1365.00 | 465.00 | 3.01985936*E* – 11 | ↑ |
| AGDE | 1175.00 | 655.00 | 1.24770538*E* – 04 | ↑ |
| DE_WOA | 1177.00 | 653.00 | 1.10577260*E* – 04 | ↑ |

The sign "↑" and "≈" means that DPGSK is significantly superior and similar to the compared competitor.

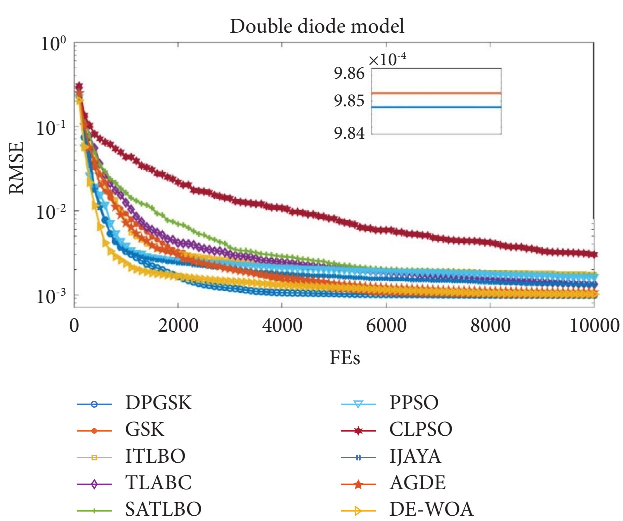


Figure 6: Convergence curves different algorithms in the DDM.

respectively. Although IGSK2 gets the optimum value of 4.95508657E-17 in the SDM, DPGSK's value (5.01330110E-17) is only a little short of IGSK2.

Summarizing the above comparisons, we can see that DPGSK obtains the optimal values the most often. When it does not, the difference between its value and the best value is very slight. IGSK2 obtains the optimal value the second most often, GSK follows, and IGSK1 is at the end. Overall, DPGSK proves to be more effective in identifying accurate and reliable parameters for these PV models.

*5.5.2. Analysis of the Test Results.* The test results in Table 25 show that the $R^+$ exceeds the $R^-$ for all models. In the SDM, the significance indicator exceeds 0.05 only for IGSK1, and thus, the other two algorithms are significantly worse than DPGSK. In the DDM, the $p$-values of GSK and IGSK2 exceed 0.05, indicating they are statistically comparable to DPGSK. In the other three PV modules, the significance indicators are considerably less than 0.05, meaning that DPGSK is significantly superior to the rest algorithms. Considering the above, DPGSK is statistically better than GSK, IGSK1, and IGSK2.

*5.6. Discussions.* In this paper, we boost the efficacy of the original GSK algorithm using a dual-population evolution strategy. The resultant DPGSK algorithm to identify the PV models' parameters is compared with various excellent metaheuristics in five models. The effect of different components on DPGSK is also investigated. From the results, we have reached the following summations:

(1) The characteristic curves of I-V and P-V show that DPGSK obtains superior accuracy and reliability in parameter identification. The IAE values for DPGSK in the five PV models are 0.01769439, 0.01759995, 0.04153981, 0.06429210, and 0.27460349, respectively, which are all the best compared with other algorithms.

(2) The RMSE values show that DPGSK achieves optimal values in the five models, and in particular, it outperforms others evidently in terms of standard deviation. Besides, the test $R^+$, $R^-$, and $p$ values present that DPGSK gets the most accurate values and shows

Table 12: Parameter identification results of the Photowatt-PW201 module.

| Algorithm | Parameter | | | | |
|---|---|---|---|---|---|
| | $I_{ph}$ (A) | $I_{sd}$ ($\mu$A) | $R_s$ ($\Omega$) | $R_{sh}$ ($\Omega$) | $n$ |
| DPGSK | 1.03051430 | 3.48226306 | 1.20127100 | 981.98224632 | 48.64283503 |
| GSK | 1.03051431 | 3.48226099 | 1.20127104 | 981.98120353 | 48.64283278 |
| ITLBO | 1.03044768 | 3.43239211 | 1.20299680 | 985.81188317 | 48.58697983 |
| SATLBO | 1.03066993 | 2.61812262 | 1.23945153 | 952.61293357 | 47.56009632 |
| TLABC | 1.03059985 | 3.41535302 | 1.20283782 | 957.61637732 | 48.56901287 |
| IJAYA | 1.03067358 | 3.32748556 | 1.20534996 | 923.06854887 | 48.47141869 |
| PPSO | 1.03066227 | 3.40455344 | 1.20359921 | 956.17388108 | 48.55670692 |
| CLPSO | 1.03194503 | 4.80166061 | 1.14178462 | 753.68578258 | 49.92457911 |
| AGDE | 1.03051430 | 3.48226269 | 1.20127102 | 981.98235599 | 48.64283461 |
| DE_WOA | 1.03051401 | 3.48247551 | 1.20126216 | 982.02716996 | 48.64306864 |

Table 13: Parameter identification results of the STM6-40/36 module.

| Algorithm | Parameter | | | | |
|---|---|---|---|---|---|
| | $I_{ph}$ (A) | $I_{sd}$ ($\mu$A) | $R_s$ ($\Omega$) | $R_{sh}$ ($\Omega$) | $n$ |
| DPGSK | 1.66390478 | 1.73865689 | 0.00427377 | 15.92829400 | 1.52030292 |
| GSK | 1.66390491 | 1.73865480 | 0.00427377 | 15.92830421 | 1.52030275 |
| ITLBO | 1.66291802 | 2.32922408 | 0.00329262 | 17.67901268 | 1.55312223 |
| SATLBO | 1.66242121 | 3.24072656 | 0.00219364 | 19.81988076 | 1.59198324 |
| TLABC | 1.66496850 | 1.49591379 | 0.00474385 | 14.81882861 | 1.50398507 |
| IJAYA | 1.66566937 | 1.31619537 | 0.00500220 | 13.97331288 | 1.49035945 |
| PPSO | 1.66400834 | 1.66355701 | 0.00440936 | 15.70905258 | 1.51546361 |
| CLPSO | 1.68515659 | 1.33316783 | 0.00238545 | 14.63260110 | 1.78305059 |
| AGDE | 1.66390479 | 1.73866072 | 0.00427376 | 15.92829744 | 1.52030316 |
| DE_WOA | 1.66390477 | 1.73865738 | 0.00427377 | 15.92829743 | 1.52030295 |

Table 14: Parameter identification results of the STP6-120/36 module.

| Algorithm | Parameter | | | | |
|---|---|---|---|---|---|
| | $I_{ph}$ (A) | $I_{sd}$ ($\mu$A) | $R_s$ ($\Omega$) | $R_{sh}$ ($\Omega$) | $n$ |
| DPGSK | 7.47252993 | 2.33499503 | 0.00459463 | 22.21989009 | 1.26010347 |
| GSK | 7.47252810 | 2.33498605 | 0.00459464 | 22.22282108 | 1.26010320 |
| ITLBO | 7.47867495 | 2.48328081 | 0.00456420 | 16.93389869 | 1.26533610 |
| SATLBO | 7.55010206 | 33.20410083 | 0.00293965 | 17.73907128 | 1.52961944 |
| TLABC | 7.47266894 | 2.33243162 | 0.00459544 | 22.08141044 | 1.26001308 |
| IJAYA | 7.51783186 | 5.12186124 | 0.00417303 | 12.29917328 | 1.32886699 |
| PPSO | 7.50376792 | 2.31232586 | 0.00317927 | 20.02371401 | 1.48672583 |
| CLPSO | 7.53505228 | 4.16487988 | 0.00278201 | 15.23020319 | 1.55760973 |
| AGDE | 7.47254343 | 2.33103110 | 0.00459542 | 22.14767462 | 1.25996110 |
| DE_WOA | 7.47253093 | 2.33497159 | 0.00459464 | 22.21826350 | 1.26010264 |

the strongest robustness in searching for the global optimal solutions. It proves that the dual-population evolution strategy does raise the accuracy of GSK in solving the parameter identification of PV models.

(3) With regard to the convergence curves, DPGSK and DE_WOA have faster convergence at the beginning of the iteration. Although DE_WOA converges fastest in the DDM, STM6-40/36, and STP6-120/36, it tends to fall into local extrema. DPGSK can avoid local convergence and search for the global optimum effectively. Besides, it is worth mentioning that DPGSK can address the issue of slow convergence of the GSK algorithm in early iterations.

(4) DPGSK's overall performance is verified more comprehensively through the Friedman test. DPGSK ranks first with an average ranking of 1.40, followed by GSK, DE_WOA, AGDE, IJAYA, TLABC, PPSO, ITLBO, SATLBO, and CLPSO. The ranking results demonstrate the marked superiority of DPGSK over other algorithms in tackling this studied problem.

(5) The effect of the junior phase and the senior phase on DPGSK is analyzed. The results show that these two phases do affect the performance of DPGSK. Either component is indispensable to DPGSK. Nevertheless, the proposed dual-population evolution strategy can exhibit the power to coordinate them well.

Table 15: IAE results in the Photowatt-PW201 module.

| Item | $V_L$ (V) | $I_{L\text{measured}}$ (A) | $I_{L\text{calculated}}$ (A) | | | | | | |
|---|---|---|---|---|---|---|---|---|---|
| | | | DPGSK | GSK | ITLBO | TLABC | IJAYA | PPSO | AGDE |
| 1 | 0.1248 | 1.0315 | 1.02919209 | 1.02919208 | 1.02905920 | 1.02917072 | 1.02918849 | 1.02923011 | 1.02923011 |
| 2 | 1.8093 | 1.0300 | 1.02738435 | 1.02738436 | 1.02732835 | 1.02738979 | 1.02734233 | 1.02744658 | 1.02744658 |
| 3 | 3.3511 | 1.0260 | 1.02574214 | 1.02574214 | 1.02569285 | 1.02570863 | 1.02560225 | 1.02576310 | 1.02576310 |
| 4 | 4.7622 | 1.0220 | 1.02405399 | 1.02406101 | 1.02406176 | 1.02403615 | 1.02387760 | 1.02408867 | 1.02408867 |
| 5 | 6.0538 | 1.0180 | 1.02228341 | 1.02228341 | 1.02224939 | 1.02218680 | 1.02198398 | 1.02223779 | 1.02223779 |
| 6 | 7.2364 | 1.0155 | 1.01988740 | 1.01990740 | 1.01989398 | 1.01979923 | 1.01956222 | 1.01984925 | 1.01984925 |
| 7 | 8.3189 | 1.0140 | 1.01635081 | 1.01635081 | 1.01634184 | 1.01622066 | 1.01596271 | 1.01627036 | 1.01627036 |
| 8 | 9.3097 | 1.0100 | 1.01049143 | 1.01049143 | 1.01050210 | 1.01036154 | 1.01009951 | 1.01041151 | 1.01041151 |
| 9 | 10.2163 | 1.0035 | 1.00067876 | 1.00067876 | 1.00071461 | 1.00056341 | 1.00031699 | 1.00061378 | 1.00061378 |
| 10 | 11.0449 | 0.9880 | 0.98465335 | 0.98465335 | 0.98471834 | 0.98456668 | 0.98435574 | 0.98461667 | 0.98461667 |
| 11 | 11.8018 | 0.9630 | 0.95969741 | 0.95969741 | 0.95979128 | 0.95964995 | 0.95949003 | 0.95969740 | 0.95969740 |
| 12 | 12.4929 | 0.9255 | 0.92304876 | 0.92304876 | 0.92316502 | 0.92304371 | 0.92294136 | 0.92308508 | 0.92308508 |
| 13 | 13.1231 | 0.8725 | 0.87258816 | 0.87258817 | 0.87271422 | 0.87261959 | 0.87257006 | 0.87265070 | 0.87265070 |
| 14 | 13.6983 | 0.8075 | 0.80739213 | 0.80739013 | 0.80743031 | 0.80736470 | 0.80735418 | 0.80738205 | 0.80738205 |
| 15 | 14.2221 | 0.7265 | 0.72795782 | 0.72795783 | 0.72805795 | 0.72801921 | 0.72803047 | 0.72802144 | 0.72802144 |
| 16 | 14.6995 | 0.6345 | 0.63646618 | 0.63646619 | 0.63653731 | 0.63652005 | 0.63653864 | 0.63650849 | 0.63650849 |
| 17 | 15.1346 | 0.5345 | 0.53569607 | 0.53569608 | 0.53573580 | 0.53573308 | 0.53575082 | 0.53571142 | 0.53571142 |
| 18 | 15.5311 | 0.4275 | 0.42881615 | 0.42881616 | 0.42882779 | 0.42883256 | 0.42884801 | 0.42880600 | 0.42880600 |
| 19 | 15.8929 | 0.3185 | 0.31866266 | 0.31866267 | 0.31865925 | 0.31866529 | 0.31868219 | 0.31863952 | 0.31863952 |
| 20 | 16.2229 | 0.2085 | 0.20785712 | 0.20785712 | 0.20783547 | 0.20783778 | 0.20786289 | 0.20781823 | 0.20781823 |
| 21 | 16.5241 | 0.1010 | 0.09835421 | 0.09835421 | 0.09832938 | 0.09832420 | 0.09836545 | 0.09831560 | 0.09831560 |
| 22 | 16.7987 | −0.0080 | −0.00816934 | −0.00816935 | −0.00818905 | −0.00820433 | −0.00819923 | −0.00819817 | −0.00819817 |
| 23 | 17.0499 | −0.1110 | −0.11096845 | −0.11096845 | −0.11097591 | −0.11103032 | −0.11090721 | −0.11097918 | −0.11097918 |
| 24 | 17.2793 | −0.2090 | −0.20910752 | −0.20910754 | −0.20910699 | −0.20914695 | −0.20910487 | −0.20910337 | −0.20910337 |
| 25 | 17.4885 | −0.3030 | −0.30202238 | −0.30202236 | −0.30198950 | −0.30204274 | −0.30187032 | −0.30197816 | −0.30197816 |
| | ∑ IAE | — | **0.04153981** | 0.04156890 | 0.04184719 | 0.04171346 | 0.04161306 | 0.04157073 | 0.04157073 |

The optimum values are highlighted in bold.

Table 16: IAE results in the STM6-40/36 module.

| Item | $V_L$ (V) | $I_{L\text{measured}}$ (A) | $I_{L\text{calculated}}$ (A) | | | | | | |
|---|---|---|---|---|---|---|---|---|---|
| | | | DPGSK | GSK | ITLBO | TLABC | IJAYA | PPSO | AGDE |
| 1 | 0.0000 | 1.6630 | 1.66345813 | 1.66345826 | 1.66260805 | 1.66443537 | 1.66507301 | 1.66354109 | 1.66345815 |
| 2 | 0.1180 | 1.6630 | 1.66325224 | 1.66325237 | 1.66242248 | 1.66421410 | 1.66483839 | 1.66333233 | 1.66325226 |
| 3 | 2.2370 | 1.6610 | 1.65955120 | 1.65955133 | 1.65908545 | 1.66023736 | 1.66062210 | 1.65957999 | 1.65955121 |
| 4 | 5.4340 | 1.6530 | 1.65391446 | 1.65391460 | 1.65398860 | 1.65418895 | 1.65421589 | 1.65386715 | 1.65391448 |
| 5 | 7.2600 | 1.6500 | 1.65056580 | 1.65056595 | 1.65093009 | 1.65061376 | 1.65044382 | 1.65047762 | 1.65056582 |
| 6 | 9.6800 | 1.6450 | 1.64543044 | 1.64543058 | 1.64610666 | 1.64521365 | 1.64481498 | 1.64529874 | 1.64543045 |
| 7 | 11.5900 | 1.6400 | 1.63923405 | 1.63923420 | 1.63999761 | 1.63888800 | 1.63838498 | 1.63909183 | 1.63923407 |
| 8 | 12.6000 | 1.6360 | 1.63371510 | 1.63371525 | 1.63440865 | 1.63336092 | 1.63286405 | 1.63358524 | 1.63371511 |
| 9 | 13.3700 | 1.6290 | 1.62728848 | 1.62728863 | 1.62784771 | 1.62697130 | 1.62652647 | 1.62718088 | 1.62728850 |
| 10 | 14.0900 | 1.6190 | 1.61831518 | 1.61831533 | 1.61867332 | 1.61807425 | 1.61772795 | 1.61824074 | 1.61831519 |
| 11 | 14.8800 | 1.5970 | 1.60306738 | 1.60306753 | 1.60312097 | 1.60295914 | 1.60278898 | 1.60304385 | 1.60306739 |
| 12 | 15.5900 | 1.5810 | 1.58158500 | 1.58158515 | 1.58131434 | 1.58163074 | 1.58168525 | 1.58161748 | 1.58158501 |
| 13 | 16.4000 | 1.5420 | 1.54232746 | 1.54232760 | 1.54171614 | 1.54254961 | 1.54292624 | 1.54242399 | 1.54232746 |
| 14 | 16.7100 | 1.5240 | 1.52122498 | 1.52122512 | 1.52052881 | 1.52149721 | 1.52200675 | 1.52134082 | 1.52122499 |
| 15 | 16.9800 | 1.5000 | 1.49920573 | 1.49920587 | 1.49847526 | 1.49950443 | 1.50012831 | 1.49933327 | 1.49920574 |
| 16 | 17.1300 | 1.4850 | 1.48527115 | 1.48527129 | 1.48454267 | 1.48557516 | 1.48626024 | 1.48540239 | 1.48527116 |
| 17 | 17.3200 | 1.4650 | 1.46564322 | 1.46564336 | 1.46494367 | 1.46594192 | 1.46670030 | 1.46577552 | 1.46564323 |
| 18 | 17.9100 | 1.3880 | 1.38759935 | 1.38759947 | 1.38723486 | 1.38776734 | 1.38869950 | 1.38770062 | 1.38759937 |
| 19 | 19.0800 | 1.1180 | 1.11837212 | 1.11837216 | 1.12017631 | 1.11756378 | 1.11833822 | 1.11819130 | 1.11837216 |
| 20 | 21.0200 | 0.0000 | −0.00002133 | −0.00002166 | −0.00039888 | 0.00020655 | 0.00005339 | −0.00002328 | −0.00002136 |
| | ∑ IAE | — | **0.06429210** | 0.06432185 | 0.06740885 | 0.06733509 | 0.07094699 | 0.06453392 | 0.06436733 |

The optimum values are highlighted in bold.

Table 17: IAE results in the STP6-120/36 module.

| Item | $V_L$ (V) | $I_{L\text{measured}}$ (A) | $I_{L\text{calculated}}$ (A) | | | | | | |
|---|---|---|---|---|---|---|---|---|---|
| | | | DPGSK | GSK | ITLBO | TLABC | IJAYA | PPSO | AGDE |
| 1 | 0.0000 | 7.4800 | 7.47698179 | 7.47698019 | 7.47665638 | 7.47111081 | 7.51527601 | 7.50310413 | 7.47098999 |
| 2 | 9.0600 | 7.4500 | 7.45253756 | 7.45253743 | 7.45451827 | 7.45259805 | 7.48530660 | 7.49450105 | 7.45251333 |
| 3 | 9.4700 | 7.4200 | 7.44934550 | 7.44934543 | 7.45111948 | 7.44940349 | 7.48101491 | 7.48368056 | 7.44932094 |
| 4 | 10.3200 | 7.4400 | 7.43909225 | 7.43909232 | 7.44039457 | 7.43914567 | 7.46785784 | 7.47142399 | 7.43906828 |
| 5 | 11.1700 | 7.4100 | 7.42026504 | 7.42026524 | 7.42101522 | 7.42031503 | 7.44495300 | 7.44796198 | 7.42024411 |
| 6 | 11.8100 | 7.3800 | 7.39587321 | 7.39587350 | 7.39613741 | 7.39592154 | 7.41644421 | 7.40403264 | 7.39585681 |
| 7 | 12.3600 | 7.3700 | 7.36326491 | 7.36326527 | 7.36305632 | 7.36331247 | 7.37943806 | 7.36924502 | 7.36325428 |
| 8 | 12.7400 | 7.3400 | 7.33148326 | 7.33148365 | 7.33091921 | 7.33153057 | 7.34413104 | 7.33486735 | 7.33147771 |
| 9 | 13.1600 | 7.2900 | 7.28413020 | 7.28413063 | 7.28315199 | 7.28417735 | 7.29245408 | 7.28686643 | 7.28413125 |
| 10 | 13.5900 | 7.2300 | 7.21776129 | 7.21776173 | 7.21634963 | 7.21780812 | 7.22130851 | 7.21603695 | 7.21776995 |
| 11 | 14.1700 | 7.1000 | 7.08813761 | 7.08813803 | 7.08617271 | 7.08818289 | 7.08511764 | 7.08444912 | 7.08815694 |
| 12 | 14.5800 | 6.9700 | 6.95844943 | 6.95844981 | 6.95616503 | 6.95849205 | 6.95118750 | 6.95847554 | 6.95847554 |
| 13 | 14.9300 | 6.8300 | 6.81486058 | 6.81486089 | 6.81239172 | 6.81489929 | 6.80465661 | 6.74814273 | 6.81489101 |
| 14 | 15.3900 | 6.5800 | 6.56792998 | 6.56793018 | 6.56540330 | 6.56796057 | 6.55542580 | 6.50237572 | 6.56796260 |
| 15 | 15.7100 | 6.3600 | 6.34872814 | 6.34872825 | 6.34632033 | 6.34875084 | 6.33602884 | 6.28894274 | 6.34875907 |
| 16 | 16.0800 | 6.0000 | 6.03749323 | 6.03749322 | 6.03541018 | 6.03750464 | 6.02623996 | 5.99024242 | 6.03751827 |
| 17 | 16.3400 | 5.7500 | 5.77681472 | 5.77681465 | 5.77508163 | 5.77681719 | 5.76764593 | 5.74212427 | 5.77683304 |
| 18 | 16.7600 | 5.2700 | 5.27376618 | 5.27376604 | 5.27278276 | 5.27375386 | 5.26946723 | 5.26494555 | 5.27376968 |
| 19 | 16.9000 | 5.0700 | 5.08193494 | 5.08193479 | 5.08123945 | 5.08191802 | 5.07951765 | 5.08277576 | 5.08193271 |
| 20 | 17.1000 | 4.7900 | 4.78583409 | 4.78583395 | 4.78556827 | 4.78581135 | 4.78615088 | 4.80074242 | 4.78582332 |
| 21 | 17.2500 | 4.5600 | 4.54629057 | 4.54629048 | 4.54635205 | 4.54626429 | 4.54858123 | 4.57184242 | 4.54627337 |
| 22 | 17.4100 | 4.2900 | 4.27393013 | 4.27393010 | 4.27433549 | 4.27390109 | 4.27813192 | 4.31024324 | 4.27390624 |
| 23 | 17.6500 | 3.8300 | 3.83228334 | 3.83228345 | 3.83317162 | 3.83225270 | 3.83869284 | 3.88291542 | 3.83225035 |
| 24 | 19.2100 | 0.0000 | 0.00116402 | 0.00116712 | 0.00184104 | 0.00124967 | -0.02787477 | 0.00762152 | 0.00115712 |
| | $\sum$ IAE | — | **0.27460349** | 0.27460538 | 0.28986916 | 0.28038683 | 0.48079071 | 0.64413128 | 0.28045679 |

The optimum values are highlighted in bold.

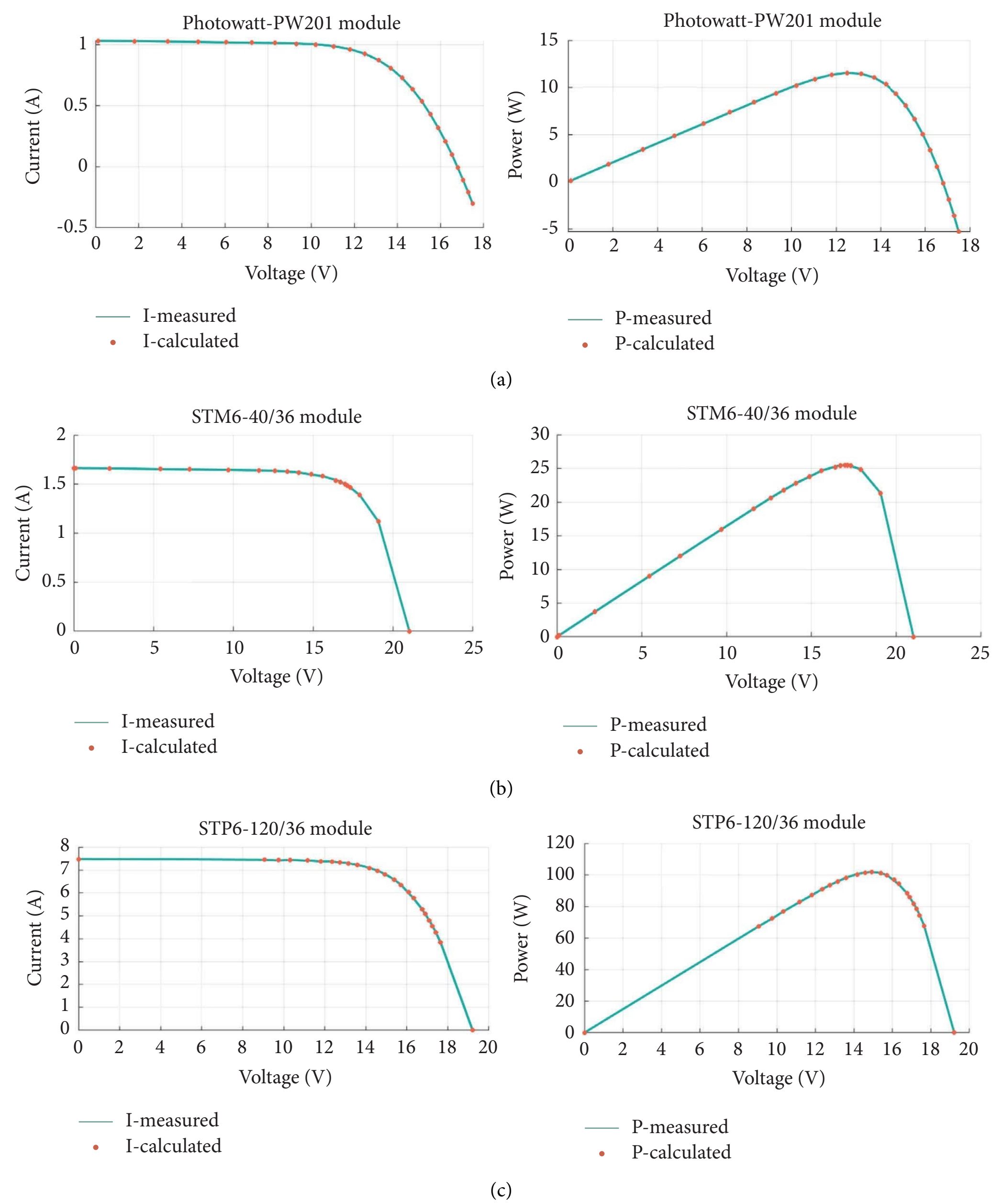


Figure 7: Characteristic curves of DPGSK: (a) Photowatt-PW201 module, (b) STM6-40/36 module, and (c) STP6-120/36 module.

Table 18: RMSE values in the Photowatt-PW201 module.

| Algorithm | RMSE | | | |
|---|---|---|---|---|
| | Best | Worst | Mean | Std |
| DPGSK | **2.42507487E – 03** | **2.42507487E – 03** | **2.42507487E – 03** | **4.75324029E – 17** |
| GSK | **2.42507487E – 03** | 2.43124074*E* – 03 | 2.42529952*E* – 03 | 1.12527868*E* – 06 |
| ITLBO | 2.42613506*E* – 03 | 6.78078310*E* – 03 | 2.83290424*E* – 03 | 8.11128363*E* – 04 |
| SATLBO | 2.43587695*E* – 03 | 6.03229203*E* – 03 | 3.04534170*E* – 03 | 8.69364652*E* – 04 |
| TLABC | 2.42618247*E* – 03 | 4.05234846*E* – 03 | 2.67703585*E* – 03 | 3.83080237*E* – 04 |
| IJAYA | 2.42566534*E* – 03 | 2.95825827*E* – 03 | 2.53272931*E* – 03 | 1.44953051*E* – 04 |
| PPSO | 2.42508316*E* – 03 | 8.83755053*E* – 03 | 2.94600003*E* – 03 | 1.24746322*E* – 03 |
| CLPSO | 2.83408533*E* – 03 | 6.75827193*E* – 03 | 4.01222813*E* – 03 | 9.56232818*E* – 04 |
| AGDE | **2.42507487E – 03** | 2.42507628*E* – 03 | 2.42507492*E* – 03 | 2.56868962*E* – 10 |
| DE_WOA | 2.42507489*E* – 03 | 3.54660632*E* – 03 | 2.56291129*E* – 03 | 2.64120863*E* – 04 |

The optimum values are highlighted in bold.

Table 19: RMSE values in the STM6-40/36 module.

| Algorithm | RMSE | | | |
|---|---|---|---|---|
| | Best | Worst | Mean | Std |
| DPGSK | **1.72981371E – 03** | **1.72981371E – 03** | **1.72981371E – 03** | **6.69268329E – 18** |
| GSK | **1.72981371E – 03** | 1.72981372E – 03 | **1.72981371E – 03** | 1.50670485E – 12 |
| ITLBO | 1.80302370E – 03 | 5.04532930E – 02 | 5.08181795E – 03 | 8.64964315E – 03 |
| SATLBO | 2.00426673E – 03 | 2.98051206E – 02 | 8.68645469E – 03 | 7.72801077E – 03 |
| TLABC | 1.73011828E – 03 | 6.71432512E – 02 | 5.15375645E – 03 | 1.18096851E – 02 |
| IJAYA | 1.80656350E – 03 | 3.38695808E – 03 | 2.69248270E – 03 | 4.76741812E – 04 |
| PPSO | 1.73296413E – 03 | 3.08607469E – 02 | 4.78248606E – 03 | 5.06632794E – 03 |
| CLPSO | 5.51270979E – 03 | 2.82327010E – 02 | 1.59673399E – 02 | 7.07623601E – 03 |
| AGDE | **1.72981371E – 03** | 1.90393613E – 03 | 1.73951550E – 03 | 3.26588994E – 05 |
| DE_WOA | **1.72981371E – 03** | **1.72981371E – 03** | **1.72981371E – 03** | 7.83732302E – 13 |

The optimum values are highlighted in bold.

Table 20: RMSE values in the STP6-120/36 module.

| Algorithm | RMSE | | | |
|---|---|---|---|---|
| | Best | Worst | Mean | Std |
| DPGSK | **1.66006031E – 02** | **1.66006031E – 02** | **1.66006031E – 02** | **3.64215013E – 16** |
| GSK | **1.66006031E – 02** | 1.66006379E – 02 | 1.66006043E – 02 | 6.34321846E – 09 |
| ITLBO | 1.66026542E – 02 | 1.82932081E – 01 | 4.09561836E – 02 | 3.36881282E – 02 |
| SATLBO | 1.67283597E – 02 | 5.94301196E – 02 | 4.09933264E – 02 | 1.18675783E – 02 |
| TLABC | 1.66007077E – 02 | 2.27284953E – 01 | 3.51585815E – 02 | 4.39960971E – 02 |
| IJAYA | 1.73920763E – 02 | 2.74919656E – 02 | 2.09806168E – 02 | 3.00496502E – 03 |
| PPSO | 1.66391981E – 02 | 1.14874892E – 01 | 4.06962594E – 02 | 1.85185406E – 02 |
| CLPSO | 3.52931825E – 02 | 8.67923901E – 01 | 1.77656627E – 01 | 1.93537380E – 01 |
| AGDE | **1.66006031E – 02** | 1.34812942E – 01 | 2.06460413E – 02 | 2.15653571E – 02 |
| DE_WOA | **1.66006031E – 02** | 1.66007829E – 02 | 1.66006139E – 02 | 4.10680224E – 08 |

Table 21: $R^+$, $R^-$, and $p$ values of Wilcoxon's rank-sum test for the RMSE values of the DPGSK vs. other algorithms for the Photowatt-PW201 module.

| DPGSK vs. | $R^+$ | $R^-$ | $p$ value | Sig. |
|---|---|---|---|---|
| GSK | 1365.00 | 465.00 | 2.96913841E – 11 | ↑ |
| ITLBO | 1365.00 | 465.00 | 2.96913841E – 11 | ↑ |
| SATLBO | 1365.00 | 465.00 | 2.96913841E – 11 | ↑ |
| TLABC | 1365.00 | 465.00 | 2.96913841E – 11 | ↑ |
| IJAYA | 1365.00 | 465.00 | 2.96913841E – 11 | ↑ |
| PPSO | 1365.00 | 465.00 | 2.96913841E – 11 | ↑ |
| CLPSO | 1365.00 | 465.00 | 2.96913841E – 11 | ↑ |
| AGDE | 1327.50 | 502.50 | 1.09035598E – 09 | ↑ |
| DE_WOA | 1365.00 | 465.00 | 2.96913841E – 11 | ↑ |

The sign "↑" means that DPGSK is significantly superior to the compared competitor.

Table 22: $R^+$, $R^-$, and $p$ values of Wilcoxon's rank-sum test for the RMSE values of the DPGSK vs. other algorithms for the STM6-40/36 module.

| DPGSK vs. | $R^+$ | $R^-$ | $p$ value | Sig. |
|---|---|---|---|---|
| GSK | 1356.50 | 473.50 | 4.42956883E – 11 | ↑ |
| ITLBO | 1365.00 | 465.00 | 1.98787859E – 11 | ↑ |
| SATLBO | 1365.00 | 465.00 | 1.98787859E – 11 | ↑ |
| TLABC | 1365.00 | 465.00 | 1.98787859E – 11 | ↑ |
| IJAYA | 1365.00 | 465.00 | 1.98787859E – 11 | ↑ |
| PPSO | 1365.00 | 465.00 | 1.98787859E – 11 | ↑ |
| CLPSO | 1365.00 | 465.00 | 1.98787859E – 11 | ↑ |
| AGDE | 1365.00 | 465.00 | 1.98787859E – 11 | ↑ |
| DE_WOA | 1341.00 | 489.00 | 2.03566531E – 10 | ↑ |

The sign "↑" means that DPGSK is significantly superior to the compared competitor.

Table 23: $R^+$, $R^-$, and $p$ values of Wilcoxon's rank-sum test for the RMSE values of the DPGSK vs. other algorithms for the STP6-120/36 module.

| DPGSK vs. | $R^+$ | $R^-$ | $p$ value | Sig. |
|---|---|---|---|---|
| GSK | 1363.00 | 467.00 | $3.29327551E-11$ | ↑ |
| ITLBO | 1365.00 | 465.00 | $2.69269726E-11$ | ↑ |
| SATLBO | 1365.00 | 465.00 | $2.69269726E-11$ | ↑ |
| TLABC | 1365.00 | 465.00 | $2.69269726E-11$ | ↑ |
| IJAYA | 1365.00 | 465.00 | $2.69269726E-11$ | ↑ |
| PPSO | 1365.00 | 465.00 | $2.69269726E-11$ | ↑ |
| CLPSO | 1365.00 | 465.00 | $2.69269726E-11$ | ↑ |
| AGDE | 1365.00 | 465.00 | $2.69269726E-11$ | ↑ |
| DE_WOA | 1354.50 | 475.50 | $7.59190233E-11$ | ↑ |

The sign "↑" means that DPGSK is significantly superior to the compared competitor.

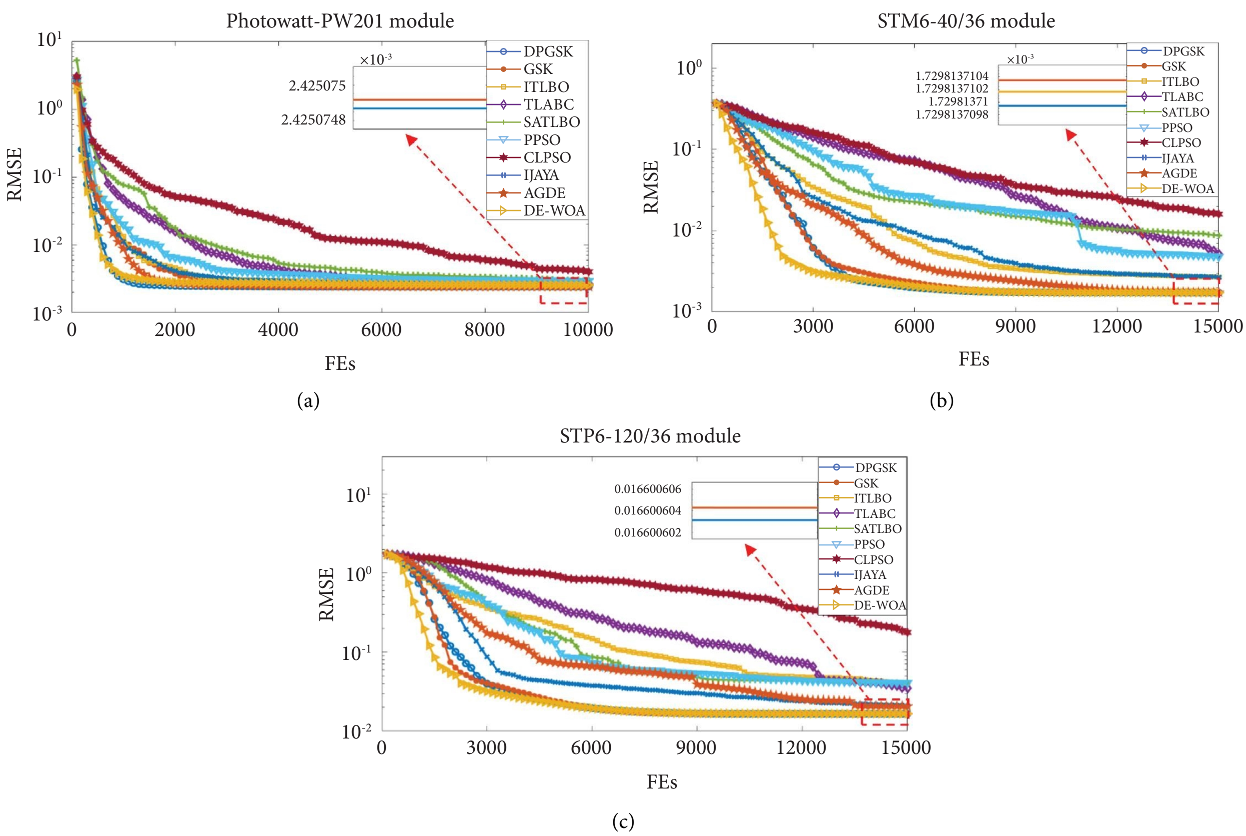


Figure 8: Convergence curves: (a) Photowatt-PW201 module, (b) STM6-40/36 module, and (c) STP6-120/36 module.

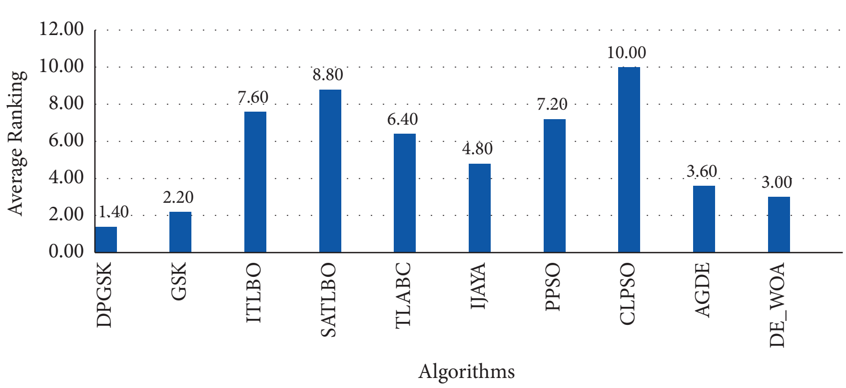


Figure 9: Friedman test result.

Table 24: RMSE values for different variants of DPGSK.

| Model | Algorithm | RMSE | | | |
|---|---|---|---|---|---|
| | | Best | Worst | Mean | Std |
| SDM | DPGSK | **9.86021878E – 04** | **9.86021878E – 04** | **9.86021878E – 04** | 5.01330110$E$ – 17 |
| | GSK | **9.86021878E – 04** | 9.86021881$E$ – 04 | **9.86021878E – 04** | 5.77198278$E$ – 13 |
| | IGSK1 | **9.86021878E – 04** | 1.14970749$E$ – 03 | 1.00334452$E$ – 03 | 3.09917403$E$ – 05 |
| | IGSK2 | **9.86021878E – 04** | **9.86021878E – 04** | **9.86021878E – 04** | **4.95508657E – 17** |
| DDM | DPGSK | 9.82484859$E$ – 04 | **9.87885272E – 04** | **9.84815569E – 04** | **1.68677548E – 06** |
| | GSK | 9.82681198$E$ – 04 | 9.91166708$E$ – 04 | 9.85246463$E$ – 04 | 1.78610712$E$ – 06 |
| | IGSK1 | 9.83129226$E$ – 04 | 3.35318293$E$ – 03 | 1.69916657$E$ – 03 | 5.92923212$E$ – 04 |
| | IGSK2 | **9.82484852E – 04** | 9.90885053$E$ – 04 | 9.85386108$E$ – 04 | 1.82893145$E$ – 06 |
| Photowatt-PW201 | DPGSK | **2.42507487E – 03** | **2.42507487E – 03** | **2.42507487E – 03** | **4.75324029E – 17** |
| | GSK | **2.42507487E – 03** | 2.43124074$E$ – 03 | 2.42529952$E$ – 03 | 1.12527868$E$ – 06 |
| | IGSK1 | **2.42507487E – 03** | 2.43852468$E$ – 03 | 2.42617462$E$ – 03 | 2.72385502$E$ – 06 |
| | IGSK2 | **2.42507487E – 03** | 2.42774735$E$ – 03 | 2.42516515$E$ – 03 | 4.87738798$E$ – 07 |
| STM6-40/36 | DPGSK | **1.72981371E – 03** | **1.72981371E – 03** | **1.72981371E – 03** | **6.69268329E – 18** |
| | GSK | **1.72981371E – 03** | 1.72981372$E$ – 03 | **1.72981371E – 03** | 1.50670485$E$ – 12 |
| | IGSK1 | 1.73191719$E$ – 03 | 7.07659606$E$ – 03 | 3.38453446$E$ – 03 | 1.41010667$E$ – 03 |
| | IGSK2 | **1.72981371E – 03** | **1.72981371E – 03** | **1.72981371E – 03** | 2.49962266$E$ – 15 |
| STP6-120/36 | DPGSK | **1.66006031E – 02** | **1.66006031E – 02** | **1.66006031E – 02** | **3.64215013E – 16** |
| | GSK | **1.66006031E – 02** | 1.66006379$E$ – 02 | 1.66006043$E$ – 02 | 6.34321846$E$ – 09 |
| | IGSK1 | 1.66333141$E$ – 02 | 3.40593689$E$ – 02 | 2.35744620$E$ – 02 | 6.13100930$E$ – 03 |
| | IGSK2 | **1.66006031E – 02** | 1.66026785$E$ – 02 | 1.66006723$E$ – 02 | 3.78914430$E$ – 07 |

The optimum values are highlighted in bold.

Table 25: $R^+$, $R^-$, and $p$ values of Wilcoxon's rank-sum test for the RMSE values of the DPGSK vs. its variants for the five PV models.

| Model | DPGSK vs. | $R^+$ | $R^-$ | $p$ value | Sig. |
|---|---|---|---|---|---|
| SDM | GSK | 1355.50 | 474.50 | 7.74308961$E$ – 11 | ↑ |
| | IGSK1 | 1365 | 465 | 3.01418492$E$ – 11 | ↑ |
| | IGSK2 | 954 | 875 | 5.64171398$E$ – 01 | ≈ |
| DDM | GSK | 974.00 | 856.00 | 3.87099778$E$ – 01 | ≈ |
| | IGSK1 | 1326 | 504 | 1.28703830$E$ – 09 | ↑ |
| | IGSK2 | 948 | 882 | 6.30876292$E$ – 01 | ≈ |
| Photowatt-PW201 | GSK | 1365.00 | 465.00 | 2.96913841$E$ – 11 | ↑ |
| | IGSK1 | 1346.5 | 483.5 | 1.82527310$E$ – 10 | ↑ |
| | IGSK2 | 1167 | 663 | 1.95503446$E$ – 04 | ↑ |
| STM6-40/36 | GSK | 1356.50 | 473.50 | 4.42956883$E$ – 11 | ↑ |
| | IGSK1 | 1365 | 465 | 1.98787859$E$ – 11 | ↑ |
| | IGSK2 | 1346 | 484 | 8.29091595$E$ – 11 | ↑ |
| STP6-120/36 | GSK | 1363.00 | 467.00 | 3.29327551$E$ – 11 | ↑ |
| | IGSK1 | 1365 | 465 | 2.69269726$E$ – 11 | ↑ |
| | IGSK2 | 1245 | 585 | 8.06050812$E$ – 07 | ↑ |

The signs "↑" and "≈" mean that DPGSK is significantly superior and similar to the compared competitor, respectively.

Namely, both exploration and exploitation can be balanced well in DPGSK.

## 6. Conclusions

Parameter identification is one of the most critical problems of PV system modeling and adopting an accurate and effective algorithm to solve it is notably necessary. In this paper, a dual-population GSK (DPGSK) is suggested to tackle it. Based on the GSK algorithm, a dual-population evolution strategy is designed to balance the search between exploration and exploitation. The whole population splits randomly into two even subpopulations, one of which performs the junior phase while the other executes the senior phase. Five typical PV models are used to confirm the effectiveness of DPGSK. The effect of different components including the junior and the senior on the performance of DPGSK is also investigated. Comparative simulation results reveal that with the powerful assistance of the dual-population evolution strategy, DPGSK overcomes the shortcoming of slow convergence of GSK effectively and enhances the population diversity and convergence rate significantly to search for the global optimum. Besides, it achieves the overall best RMSE values and IAE values compared with other peer algorithms. It is further confirmed by both Wilcoxon's rank-sum test and Friedman test, indicating that DPGSK has strong competitiveness in accuracy and robustness in tackling the PV models' parameter identification problem. Moreover, either component is indispensable to DPGSK.

On the other hand, we also found that DPGSK's convergence is still not fast enough, as DE_WOA beats it at the beginning of the iteration. Thus, in future work, it is desirable to further heighten its convergence with the help of other strategies such as the population size reduction technique [64], quadratic interpolation [65], and reinforcement learning [66, 67]. In addition, we will test the suggested DPGSK algorithm's performance in more PV models and further ameliorate it to tackle more power system operation problems.

## Data Availability

The data are available upon request.

## Conflicts of Interest

The authors declare that they have no conflicts of interest.

## Acknowledgments

This research was funded by the Natural Science Foundation of Guizhou Province (QiankeheBasic-ZK[2022]General121), the National Natural Science Foundation of China (52167007), the Open Project Program of Fujian Provincial Key Laboratory of Intelligent Identification and Control of Complex Dynamic System (2022A0008), the Innovation Foundation of Guizhou University (GuiDaKanCha (2022) 03), and the Modern Power System and Its Digital Technology Engineering Research Center (QianJiaoJi (2022) 043).

## References

[1] Q. Niu, L. Zhang, and K. Li, "A biogeography-based optimization algorithm with mutation strategies for model parameter estimation of solar and fuel cells," *Energy Conversion and Management*, vol. 86, pp. 1173–1185, 2014.

[2] S. Ahmadi, H. Ghaebi, and A. Shokri, "A comprehensive thermodynamic analysis of a novel CHP system based on SOFC and APC cycles," *Energy*, vol. 186, Article ID 115899, 2019.

[3] F. Hamrang, A. Shokri, S. M. S. Mahmoudi, B. Ehghaghi, and M. A. Rosen, "Performance analysis of a new electricity and freshwater production system based on an integrated gasification combined cycle and multi- effect desalination," *Sustainability*, vol. 12, no. 19, p. 7996, 2020.

[4] S. Gude and K. C. Jana, "Parameter extraction of photovoltaic cell using an improved cuckoo search optimization," *Solar Energy*, vol. 204, pp. 280–293, 2020.

[5] G. K. Singh, "Solar power generation by PV (photovoltaic) technology: a review," *Energy*, vol. 53, pp. 1–13, 2013.

[6] B. M. Ziapour, M. Saadat, V. Palideh, and S. Afzal, "Power generation enhancement in a salinity-gradient solar pond power plant using thermoelectric generator," *Energy Conversion and Management*, vol. 136, pp. 283–293, 2017.

[7] A. R. Jordehi, "Parameter estimation of solar photovoltaic (PV) cells: a review," *Renewable and Sustainable Energy Reviews*, vol. 61, pp. 354–371, 2016.

[8] B. Neveu, M. de la Gorce, P. Monasse, and G. Trombettoni, "A generic interval branch and bound algorithm for parameter estimation," *Journal of Global Optimization*, vol. 73, no. 3, pp. 515–535, 2019.

[9] H. Chen, S. Jiao, M. Wang, A. A. Heidari, and X. Zhao, "Parameters identification of photovoltaic cells and modules using diversification-enriched Harris hawks optimization with chaotic drifts," *Journal of Cleaner Production*, vol. 244, Article ID 118778, 2020.

[10] M. Chegaar, Z. Ouennoughi, and A. Hoffmann, "A new method for evaluating illuminated solar cell parameters," *Solid-State Electronics*, vol. 45, no. 2, pp. 293–296, 2001.

[11] H. M. Waly, H. Z. Azazi, D. S. M. Osheba, and A. E. El-Sabbe, "Parameters extraction of photovoltaic sources based on experimental data," *IET Renewable Power Generation*, vol. 13, no. 9, pp. 1466–1473, 2019.

[12] A. Ortiz-Conde, F. Garciasanchez, and J. Muci, "New method to extract the model parameters of solar cells from the explicit analytic solutions of their illuminated characteristics," *Solar Energy Materials and Solar Cells*, vol. 90, no. 3, pp. 352–361, 2006.

[13] D. Chan, J. R. Phillips, and J. Phang, "A comparative study of extraction methods for solar cell model parameters," *Solid-State Electronics*, vol. 29, no. 3, pp. 329–337, 1986.

[14] H. Saleem and S. Karmalkar, "An analytical method to extract the physical parameters of a solar cell from four points on the illuminated $J{-}V$ curve," *IEEE Electron Device Letters*, vol. 30, no. 4, pp. 349–352, 2009.

[15] L. E. Peñaranda Chenche, O. S. Hernandez Mendoza, E. P. Bandarra Filho, S. Oscar, and F. Bandarra, "Comparison of four methods for parameter estimation of mono-and multi-junction photovoltaic devices using experimental data," *Renewable and Sustainable Energy Reviews*, vol. 81, pp. 2823–2838, 2018.

[16] N. T. Tong and W. Pora, "A parameter extraction technique exploiting intrinsic properties of solar cells," *Applied Energy*, vol. 176, pp. 104–115, 2016.

[17] A. A. Cardenas, M. Carrasco, F. Mancilla-David, A. Street, and R. Cárdenas, "Experimental parameter extraction in the single-diode photovoltaic model via a reduced-space search," *IEEE Transactions on Industrial Electronics*, vol. 64, no. 2, pp. 1468–1476, 2017.

[18] K. M. El-Naggar, M. R. Alrashidi, M. F. Alhajri, and A. K. Al-Othman, "Simulated Annealing algorithm for photovoltaic parameters identification," *Solar Energy*, vol. 86, no. 1, pp. 266–274, 2012.

[19] A. Chatterjee, A. Keyhani, and D. Kapoor, "Identification of photovoltaic source models," *IEEE Transactions on Energy Conversion*, vol. 26, no. 3, pp. 883–889, 2011.

[20] A. Ayang, R. Wamkeue, M. Ouhrouche et al., "Maximum likelihood parameters estimation of single-diode model of Photovoltaic generator," *Renewable Energy*, vol. 130, pp. 111–121, 2019.

[21] H. El Achouby, M. Zaimi, A. Ibral, and E. M. Assaid, "New analytical approach for modelling effects of temperature and irradiance on physical parameters of photovoltaic solar module," *Energy Conversion and Management*, vol. 177, pp. 258–271, 2018.

[22] G. Xiong, M. Shuai, and X. Hu, "Combined heat and power economic emission dispatch using improved bare-bone multi-objective particle swarm optimization," *Energy*, vol. 244, Article ID 123108, 2022.

[23] P. Lin, S. Cheng, W. Yeh, Z. Chen, and L. Wu, "Parameters extraction of solar cell models using a modified simplified

swarm optimization algorithm," *Solar Energy*, vol. 144, pp. 594–603, 2017.

[24] J. Liang, S. Ge, B. Qu et al., "Classified perturbation mutation based particle swarm optimization algorithm for parameters extraction of photovoltaic models," *Energy Conversion and Management*, vol. 203, Article ID 112138, 2020.

[25] S. M. Ebrahimi, E. Salahshour, M. Malekzadeh, and F. Gordillo, "Parameters identification of PV solar cells and modules using flexible particle swarm optimization algorithm," *Energy*, vol. 179, pp. 358–372, 2019.

[26] J. Ma, T. O. Ting, K. L. Man et al., "Parameter estimation of photovoltaic models via cuckoo search," *Journal of Applied Mathematics*, vol. 2013, pp. 362611–362618, 2013.

[27] S. Singh, S. Agrawal, A. Tiwari, I. M. Al-Helal, and D. V. Avasthi, "Modeling and parameter optimization of hybrid single channel photovoltaic thermal module using genetic algorithms," *Solar Energy*, vol. 113, pp. 78–87, 2015.

[28] M. Ismail, M. Moghavvemi, and T. Mahlia, "Characterization of PV panel and global optimization of its model parameters using genetic algorithm," *Energy Conversion and Management*, vol. 73, pp. 10–25, 2013.

[29] S. Bozorgmehri and M. Hamedi, "Modeling and optimization of anode-supported solid oxide fuel cells on cell parameters via artificial neural network and genetic algorithm," *Fuel Cells*, vol. 12, no. 1, pp. 11–23, 2012.

[30] S. C. Zhou, L. N. Xing, X. Zheng, N. Du, L. Wang, and Q. Zhang, "A self-adaptive differential evolution algorithm for scheduling a single batch-processing machine with arbitrary job sizes and release times," *IEEE Transactions on Cybernetics*, vol. 51, no. 3, pp. 1430–1442, 2021.

[31] R. V. Rao, V. J. Savsani, and D. P. Vakharia, "Teaching–Learning-Based Optimization: an optimization method for continuous non-linear large scale problems," *Information Sciences*, vol. 183, pp. 1–15, 2012.

[32] D. Oliva, M. Abd El Aziz, and A. Ella Hassanien, "Parameter estimation of photovoltaic cells using an improved chaotic whale optimization algorithm," *Applied Energy*, vol. 200, pp. 141–154, 2017.

[33] D. Oliva, E. Cuevas, and G. Pajares, "Parameter identification of solar cells using artificial bee colony optimization," *Energy*, vol. 72, pp. 93–102, 2014.

[34] G. Xiong, J. Zhang, D. Shi, X. Yuan, and M. Shin, "Application of supply-demand-based optimization for parameter extraction of solar photovoltaic models," *Complexity*, vol. 2019, pp. 1–22, 2019.

[35] F. Q. Zhao, R. Ma, and L. Wang, "A self-learning Discrete Jaya algorithm for multi-objective energy-efficient distributed No-idle flow-shop scheduling problem in heterogeneous factory system," *IEEE Transactions on Cybernetics*, vol. 52, no. 12, pp. 12675–12686, 2022.

[36] G. Xiong, J. Zhang, D. Shi, L. Zhu, and X. Yuan, "Parameter extraction of solar photovoltaic models with an either-or teaching learning based algorithm," *Energy Conversion and Management*, vol. 224, Article ID 113395, 2020.

[37] G. Xiong, J. Zhang, D. Shi, and Y. He, "Parameter extraction of solar photovoltaic models using an improved whale optimization algorithm," *Energy Conversion and Management*, vol. 174, pp. 388–405, 2018.

[38] J. P. Ram, T. S. babu, T. Dragicevic, and N. Rajasekar, "A new hybrid bee pollinator flower pollination algorithm for solar PV parameter estimation," *Energy Conversion and Management*, vol. 135, pp. 463–476, 2017.

[39] X. Chen, B. Xu, C. Mei, Y. Ding, and K. Li, "Teaching–learning–based artificial bee colony for solar photovoltaic parameter estimation," *Applied Energy*, vol. 212, pp. 1578–1588, 2018.

[40] W. L. Liu, Y. J. Gong, W. N. Chen, Z. Liu, H. Wang, and J. Zhang, "Coordinated charging scheduling of electric vehicles: a mixed-variable differential evolution approach," *IEEE Transactions on Intelligent Transportation Systems*, vol. 21, no. 12, pp. 5094–5109, 2020.

[41] D. H. Wolpert and W. G. Macready, "No free lunch theorems for optimization," *IEEE Transactions on Evolutionary Computation*, vol. 1, pp. 67–82, 1997.

[42] F. Q. Zhao, Z. S. Xu, L. Wang, N. N. Zhu, T. P. Xu, and Jonrinaldi, "A population-based iterated greedy algorithm for distributed assembly No-wait flow-shop scheduling problem," *IEEE Transactions on Industrial Informatics*, vol. 2022, pp. 3192881–12, 2022.

[43] A. W. Mohamed, A. A. Hadi, and A. K. Mohamed, "Gaining-sharing knowledge based algorithm for solving optimization problems: a novel nature-inspired algorithm," *International Journal of Machine Learning and Cybernetics*, vol. 11, no. 7, pp. 1501–1529, 2020.

[44] G. Xiong, L. Li, A. W. Mohamed, X. Yuan, and J. Zhang, "A new method for parameter extraction of solar photovoltaic models using gaining–sharing knowledge based algorithm," *Energy Reports*, vol. 7, pp. 3286–3301, 2021.

[45] M. R. Alrashidi, M. F. A Lhajri, K. M. El-Naggar, and A. K. Al-Othman, "A new estimation approach for determining the I– V characteristics of solar cells," *Solar Energy*, vol. 85, no. 7, pp. 1543–1550, 2011.

[46] A. Askarzadeh and A. Rezazadeh, "Parameter identification for solar cell models using harmony search-based algorithms," *Solar Energy*, vol. 86, no. 11, pp. 3241–3249, 2012.

[47] H. Nunes, J. Pombo, S. Mariano, M. Calado, and J. Felippe de Souza, "A new high performance method for determining the parameters of PV cells and modules based on guaranteed convergence particle swarm optimization," *Applied Energy*, vol. 211, pp. 774–791, 2018.

[48] M. G. Villalva, J. R. Gazoli, and E. R. Filho, "Comprehensive approach to modeling and simulation of photovoltaic arrays," *IEEE Transactions on Power Electronics*, vol. 24, no. 5, pp. 1198–1208, 2009.

[49] A. M. Beigi and A. Maroosi, "Parameter identification for solar cells and module using a hybrid firefly and pattern search algorithms," *Solar Energy*, vol. 171, pp. 435–446, 2018.

[50] M. Ćalasan, S. H. Abdel Aleem, and A. F. Zobaa, "On the root mean square error (RMSE) calculation for parameter estimation of photovoltaic models: a novel exact analytical solution based on Lambert W function," *Energy Conversion and Management*, vol. 210, Article ID 112716, 2020.

[51] A. Askarzadeh and A. Rezazadeh, "Artificial bee swarm optimization algorithm for parameters identification of solar cell models," *Applied Energy*, vol. 102, pp. 943–949, 2013.

[52] G. Xiong, X. Yuan, A. W. Mohamed, and J. Zhang, "Fault section diagnosis of power systems with logical operation binary gaining-sharing knowledge-based algorithm," *International Journal of Intelligent Systems*, vol. 37, no. 2, pp. 1057–1080, 2022.

[53] G. Xiong, X. Yuan, A. W. Mohamed, J. Chen, and J. Zhang, "Improved binary gaining–sharing knowledge-based algorithm with mutation for fault section location in distribution networks," *Journal of Computational Design and Engineering*, vol. 9, no. 2, pp. 393–405, 2022.

[54] A. Fathy and H. Rezk, "Parameter estimation of photovoltaic system using imperialist competitive algorithm," *Renewable Energy*, vol. 111, pp. 307–320, 2017.

[55] X. Gao, Y. Cui, J. Hu et al., "Parameter extraction of solar cell models using improved shuffled complex evolution algorithm," *Energy Conversion and Management*, vol. 157, pp. 460–479, 2018.

[56] K. Yu, J. J. Liang, B. Y. Qu, Z. Cheng, and H. Wang, "Multiple learning backtracking search algorithm for estimating parameters of photovoltaic models," *Applied Energy*, vol. 226, pp. 408–422, 2018.

[57] S. Li, W. Gong, X. Yan et al., "Parameter extraction of photovoltaic models using an improved teaching-learning-based optimization," *Energy Conversion and Management*, vol. 186, pp. 293–305, 2019.

[58] K. J. Yu, X. Chen, X. Wang, and Z. L. Wang, "Parameters identification of photovoltaic models using self-adaptive teaching-learning-based optimization," *Energy Conversion and Management*, vol. 145, pp. 233–246, 2017.

[59] M. Ghasemi, E. Akbari, A. Rahimnejad, S. E. Razavi, S. Ghavidel, and L. Li, "Phasor particle swarm optimization: a simple and efficient variant of PSO," *Soft Computing*, vol. 23, pp. 9701–9718, 2019.

[60] J. J. Liang, A. K. Qin, P. N. Suganthan, and S. Baskar, "Comprehensive learning particle swarm optimizer for global optimization of multimodal functions," *IEEE Transactions on Evolutionary Computation*, vol. 10, no. 3, pp. 281–295, 2006.

[61] K. Yu, J. J. Liang, B. Y. Qu, X. Chen, and H. Wang, "Parameters identification of photovoltaic models using an improved JAYA optimization algorithm," *Energy Conversion and Management*, vol. 150, pp. 742–753, 2017.

[62] A. W. Mohamed and A. K. Mohamed, "Adaptive guided differential evolution algorithm with novel mutation for numerical optimization," *International Journal of Machine Learning and Cybernetics*, vol. 10, no. 2, pp. 253–277, 2019.

[63] G. Xiong, J. Zhang, X. Yuan, D. Shi, Y. He, and G. Yao, "Parameter extraction of solar photovoltaic models by means of a hybrid differential evolution with whale optimization algorithm," *Solar Energy*, vol. 176, pp. 742–761, 2018.

[64] M. Z. Ali, N. H. Awad, P. N. Suganthan, and R. G. Reynolds, "An adaptive multipopulation differential evolution with dynamic population reduction," *IEEE Transactions on Cybernetics*, vol. 47, no. 9, pp. 2768–2779, 2017.

[65] G. Xiong, J. Zhang, D. Shi, L. Zhu, and X. Yuan, "Parameter extraction of solar photovoltaic models via quadratic interpolation learning differential evolution," *Sustainable Energy Fuels*, vol. 4, no. 11, pp. 5595–5608, 2020.

[66] F. Q. Zhao, X. T. Hu, L. Wang, J. L. Zhao, J. X. Tang, and Jonrinaldi, "A reinforcement learning brain storm optimization algorithm (BSO) with learning mechanism," *Knowledge-Based Systems*, vol. 235, Article ID 107645, 2022.

[67] F. Q. Zhao, S. L. Di, and L. Wang, "A hyperheuristic with Q-learning for the multiobjective energy-efficient distributed blocking flow shop scheduling problem," *IEEE Transactions on Cybernetics*, vol. 2022, pp. 1–14, Article ID 3192112, 2022.